

A lattice-based approach to the expressivity of deep ReLU neural networks

Vincent Corlay

Telecom ParisTech, Paris,

Mitsubishi Electric R&D Centre Europe, Rennes.

V.CORLAY@FR.MERCE.MEE.COM

Joseph J. Boutros *Texas A&M University, Doha.*

Philippe Ciblat *Telecom ParisTech, Paris.*

Loïc Brunel *Mitsubishi Electric R&D Centre Europe, Rennes.*

Abstract

We present new families of continuous piecewise linear (CPWL) functions in \mathbb{R}^n having a number of affine pieces growing exponentially in n . We show that these functions can be seen as the high-dimensional generalization of the triangle wave function used by Telgarsky in 2016. We prove that they can be computed by ReLU networks with quadratic depth and linear width in the space dimension. We also investigate the approximation error of one of these functions by shallower networks and prove a separation result. The main difference between our functions and other constructions is their practical interest: they arise in the scope of channel coding. Hence, computing such functions amounts to performing a decoding operation.

Keywords: Neural networks, representation, approximation, depth hierarchy, Euclidean lattices.

1. Introduction and Main Results

This paper follows two recent articles (but is self-contained), [Corlay et al. \(2018\)](#) and [Corlay et al. \(2019\)](#), where we jointly study point lattices in Euclidean space and neural networks. Our aim is twofold. Firstly, apply neural networks paradigm to find new efficient decoding algorithms. Secondly, contribute to the understanding of the efficiency of deep learning. In this work, we emphasize the second aspect and highlight a direct contribution of lattice coding theory to deep learning.

More specifically, we focus on the *expressive power of deep neural networks*. Typically, the goal of this line of research is to show that there exist functions that can be well approximated by a deep network with a polynomial number of parameters whereas an exponential number of parameters is required for a shallow network. Many results in the literature like [Montùfar et al. \(2014\)](#), [Telgarsky \(2016\)](#), [Arora et al. \(2018\)](#) utilize functions that can be addressed via “conventional methods” (i.e. not via deep neural networks): they are mostly based on one dimensional approaches. Please, see Appendices [A](#) and [B](#) for a survey on recent results on this topic and an elucidation of main techniques. Functions associated to point lattices are too complicated to be computed via conventional methods, thus illustrating the benefit of both neural networks and depth. They arise in the context of the sphere packing problem and lattices [Conway and Sloane \(1999\)](#). We argue that these functions enlighten the missing dimensional dependency in the bound of [Telgarsky \(2016\)](#). Moreover, for dimensional dependent separation bounds to hold in higher dimensions, our investigation highlights the need for sophisticated functions. Such functions can be found thanks to *dense* lattices.

Short-length error-correcting codes used to protect digital information transmission are discrete sets mainly built via Algebra: e.g. vector spaces over finite fields or modules over rings. The decoding operation in a discrete set consists in finding the closest element to a noisy received signal. This is a classification problem.

The channel coding community recently started to use deep learning techniques to tackle this classification problem. The interest in deep learning for channel coding is growing exponentially. However, the first attempts to perform decoding operations with “raw” neural networks (i.e. without using underlying graph structures of existing sub-optimal algorithms, as done in [Nachmani et al. \(2018\)](#)) were unsuccessful. For instance, an exponential number of neurons in the network is needed in [Gruber et al. \(2017\)](#) to achieve satisfactory performance. So far, it was not clear whether such a behavior is due to an unadapted learning algorithm or a consequence of a poor function class. This work is a first theoretical step towards a better understanding of the function class that should be more suitable for usage in these decoding problems.

In [Corlay et al. \(2019\)](#), we rigorously presented the duality between the decoding operation for lattices, the so-called closest vector problem (CVP), and a classification problem in the fundamental parallelotope with a CPWL function defining the decoding boundary. Preliminary results for one of the most famous root lattices, namely A_n , were also presented: for a given basis of A_n , the function defining the boundary has $\Omega(2^n)$ affine pieces. We managed to reduce the number of pieces to be computed down to a linear number via $\mathcal{O}(n^2)$ reflections with respect to the bisector hyperplane of pairs of vectors in the lattice basis. Hence, the evaluation of this decision boundary function can be performed by a ReLU network of depth $\mathcal{O}(n^2)$ and width $\mathcal{O}(n)$. We also proved that a ReLU network with only one hidden layer requires $\Omega(2^n)$ neurons to compute this function. We did not quantify the approximation error.

1.1. Main Results

In this paper, we complete the initial results of [Corlay et al. \(2019\)](#) with the following contributions:

1. We show that the CPWL boundary function f , obtained from A_n , is a n -dimensional generalization of the triangle wave function used by [Telgarsky \(2016\)](#).
2. We investigate the approximation error of f by a function g having a restricted number of pieces. We prove that, for a large enough dimension and within the fundamental parallelotope, f can be approximated by a one-neuron linear network with a negligible error. This emphasize the need for more sophisticated functions to illustrate the benefit of depth in high dimensions for a fixed size of the domain of f .
3. However, if f is not limited to this parallelotope but to a larger compact set, whose size increases exponentially with the depth of the network used for approximation, we get a separation result. Theorem 4 (with the parameter $M = n^2$) has the following consequence: there exists a function $f : \mathbb{R}^{n-1} \rightarrow \mathbb{R}$ computed by a standard ReLU neural network in $\mathcal{O}(n^2)$ layers and $\mathcal{O}(n^3)$ neurons where any function g computed by a ReLU neural network with $\leq n$ layers and $\leq 2^{n-1}$ neurons induces a L_1 approximation error $\|f - g\|_1 = \Omega(2^{(n-1)^3 - n \log_2(n)})$.
4. We present new sophisticated CPWL functions arising from root lattices D_n , $n \geq 2$, and E_n , $6 \leq n \leq 8$. The exact numbers of pieces of these functions are provided by explicit formulas. These numbers are exponential in the space dimension.

5. We show that each of these functions can be computed by a ReLU network with polynomial depth and linear width. This is achieved by *folding* the input space: i.e. we perform reflections in the input space as pre-processing. After a polynomial number of reflections, the functions can be evaluated by computing a number of affine functions growing only linearly in the space dimension.

2. Lattices, Polytopes, and the decision boundary function

This section is highly inspired from [Corlay et al. \(2019\)](#). We establish the notations and state existing results used in the sequel.

2.1. Lattices and polytopes

A lattice Λ is a discrete additive subgroup of \mathbb{R}^n . For a rank- n lattice in \mathbb{R}^n , the rows of a $n \times n$ generator matrix G constitute a basis of Λ and any lattice point x is obtained via $x = zG$, where $z \in \mathbb{Z}^n$. If needed, x also denotes the corresponding vector. Also, $\Gamma = GG^T$ is the Gram matrix (see Appendix H for more details on Γ). For a given basis $\mathcal{B} = \{b_i\}_{i=1}^n$, $\mathcal{P}(\mathcal{B})$ denotes the fundamental parallelotope of Λ and $\mathcal{V}(x)$ the Voronoi cell of a lattice point x (see Appendix H for formal definitions of these fundamental regions of a lattice). The minimum Euclidean distance of Λ is $d_{\min}(\Lambda) = 2\rho$, where ρ is the packing radius.

A vector $v \in \Lambda$ is called Voronoi vector if the half-space $\{y \in \mathbb{R}^n : y \cdot v \leq \frac{1}{2}v \cdot v\}$ has a non-empty intersection with $\mathcal{V}(0)$. The vector is said relevant if the intersection is an $n - 1$ -dimensional face of $\mathcal{V}(0)$. We denote by τ_f the number of relevant Voronoi vectors, referred to in the sequel as the *Voronoi number* of the lattice. The Voronoi number and the kissing number are equal for root lattices. The set of relevant Voronoi vectors is denoted $\tau_f(0)$. The set of lattice points having a common Voronoi facet with $x \in \Lambda$ becomes $\tau_f(x) = \tau_f(0) + x$.

Lattice decoding refers to the method of finding the closest lattice point, the closest in Euclidean distance sense. This problem is also known as the closest vector problem. Our functions are mostly studied in the compact region $\mathcal{P}(\mathcal{B})$, thus it is important to characterize $\mathcal{P}(\mathcal{B})$ as made below.

Let $\overline{\mathcal{P}}(\mathcal{B})$ be the topological closure of $\mathcal{P}(\mathcal{B})$. A k -dimensional element of $\overline{\mathcal{P}}(\mathcal{B}) \setminus \mathcal{P}(\mathcal{B})$ is referred to as k -face of $\mathcal{P}(\mathcal{B})$. There are 2^n 0-faces, called corners or vertices. This set of corners is denoted $\mathcal{C}_{\mathcal{P}(\mathcal{B})}$. Moreover, the subset of $\mathcal{C}_{\mathcal{P}(\mathcal{B})}$ obtained with $z_i = 1$ is $\mathcal{C}_{\mathcal{P}(\mathcal{B})}^{i,1}$ and $\mathcal{C}_{\mathcal{P}(\mathcal{B})}^{i,0}$ for $z_i = 0$. The remaining faces of $\mathcal{P}(\mathcal{B})$ are parallelotopes. For instance, a $n - 1$ -dimensional facet of $\mathcal{P}(\mathcal{B})$ is itself a parallelotope of dimension $n - 1$ defined by $n - 1$ vectors of \mathcal{B} . Throughout the paper, the term facet refers to a $n - 1$ -face. Also, for the sake of simplicity, $\mathcal{P}(\mathcal{B})$ refers to $\overline{\mathcal{P}}(\mathcal{B})$.

The following definition ensures optimality when decoding via the decision boundary in $\mathcal{P}(\mathcal{B})$.

Definition 1 Let \mathcal{B} be the \mathbb{Z} -basis of a rank- n lattice Λ in \mathbb{R}^n . \mathcal{B} is said *Voronoi-reduced (VR)* if, for any point $y \in \mathcal{P}(\mathcal{B})$, the closest lattice point \hat{x} to y is one of the 2^n corners of $\mathcal{P}(\mathcal{B})$, i.e. $\hat{x} = \hat{z}G$ where $\hat{z} \in \{0, 1\}^n$.

Some of the above conditions are relaxed to yield the less restrictive definition of a semi-Voronoi-reduced (SVR) basis. A rigorous understanding of this definition is not necessary to grasp the main ideas of the paper. While a SVR basis does not enable perfect decoding, it ensures the existence of a decision boundary function (described below). The formal definition of a SVR basis is provided in Appendix H.

A convex polytope (or convex polyhedron) is defined as the intersection of a finite number of half-spaces bounded by hyperplanes (Coxeter (1973)):

$$P_o = \{x \in \mathbb{R}^n : xA \leq b, A \in \mathbb{R}^{n \times m}, b \in \mathbb{R}^m\}.$$

In this paper, parallelotopes are not the only polytopes considered as we also use simplices. A i -simplex associated with $\mathcal{U} = \{u_j\}_{j=0}^i$ is given by

$$\mathcal{S}(\mathcal{U}) = \{y \in \mathbb{R}^n : y = \sum_{j=1}^i \alpha_j (u_j - u_0), \sum_{j=1}^i \alpha_j \leq 1, \alpha_j \geq 0 \forall j\}. \quad (1)$$

By abuse of terminology, the definition of (1) is maintained even if the vectors in the set \mathcal{U} are not affinely independent. In this latter case, we refer to i as the size of the simplex whereas it is its dimension otherwise. It is clear that the corners of $\mathcal{S}(\mathcal{U})$ are the $i + 1$ points of \mathcal{U} .

We say that a function $g : \mathbb{R}^{n-1} \rightarrow \mathbb{R}$ is continuous piecewise linear (CPWL) if there exists a finite set of polytopes covering \mathbb{R}^{n-1} , and g is affine over each polytope. The number of pieces of g is the number of distinct polytopes partitioning its domain.

\vee and \wedge denote respectively the maximum and the minimum operator. We define a convex (resp. concave) CPWL function formed by a set of affine functions related by the operator \vee (resp. \wedge). If $\{g_k\}$ is a set of K affine functions, the function $f = g_1 \vee \dots \vee g_K$ is CPWL and convex.

2.2. The decision boundary function

The notion of decision boundary function for a lattice was introduced in Corlay et al. (2019). Given a VR basis, after translating the point to be decoded inside $\mathcal{P}(\mathcal{B})$ to get a point $y \in \mathcal{P}(\mathcal{B})$, the decoder proceeds in estimating each z_i -component separately. The idea is to compute the position of y relative to a boundary to guess whether $z_i = 0$, i.e. the closest lattice point belongs to $\mathcal{C}_{\mathcal{P}(\mathcal{B})}^{i,0}$, or $z_i = 1$ when the closest lattice point is in $\mathcal{C}_{\mathcal{P}(\mathcal{B})}^{i,1}$. This boundary cuts $\mathcal{P}(\mathcal{B})$ into two regions. It is composed of Voronoi facets of the corner points. **For the rest of the paper, without loss of generality, the integer coordinate to be decoded is z_1 .** Also, to lighten the notations $\mathcal{C}_{\mathcal{P}(\mathcal{B})}^{1,0} = \mathcal{C}_{\mathcal{P}(\mathcal{B})}^0$ and $\mathcal{C}_{\mathcal{P}(\mathcal{B})}^{1,1} = \mathcal{C}_{\mathcal{P}(\mathcal{B})}^1$.

Any Voronoi facet is contained in a boundary hyperplane orthogonal to a vector v_j , the equation of which is:

$$\{y \in \mathbb{R}^n : y \cdot v_j - p_j = 0\}. \quad (2)$$

Any boundary hyperplane contains the Voronoi facet of a point $x \in \mathcal{C}_{\mathcal{P}(\mathcal{B})}^1$ and a point from $\tau_f(x) \cap \mathcal{C}_{\mathcal{P}(\mathcal{B})}^0$ (i.e. the Voronoi facet between x and any point in $\tau_f(x) \cap \mathcal{C}_{\mathcal{P}(\mathcal{B})}^0$ lies in a boundary hyperplane). The decision boundary cutting $\mathcal{P}(\mathcal{B})$ into two regions, with $\mathcal{C}_{\mathcal{P}(\mathcal{B})}^0$ on one side and $\mathcal{C}_{\mathcal{P}(\mathcal{B})}^1$ on the other side, is the union of these Voronoi facets. Each facet can be defined by an affine function over a compact subset of \mathbb{R}^{n-1} and the decision boundary is locally described by one of these functions.

Let $\{e_i\}_{i=1}^n$ be the canonical orthonormal basis of the vector space \mathbb{R}^n . For $y \in \mathbb{R}^n$, the i -th coordinate is $y_i = y \cdot e_i$. Denote $\tilde{y} = (y_2, \dots, y_n) \in \mathbb{R}^{n-1}$ and let $\mathcal{H} = \{h_j\}$ be the set of affine functions involved in the decision boundary. The affine boundary function $h_j : \mathbb{R}^{n-1} \rightarrow \mathbb{R}$ is

$$h_j(\tilde{y}) = y_1 = \left(p_j - \sum_{k \neq 1} y_k v_j^k \right) / v_j^1, \quad (3)$$

where p_j is a bias and v_j^k is the k -th component of vector v_j . For the sake of simplicity, in the sequel h_j shall denote the function defined in (3) or its associated hyperplane $\{y \in \mathbb{R}^n : y \cdot v_j - p_j = 0\}$ depending on the context. The following theorem shows the existence of such a boundary function for a VR or SVR basis.

Theorem 2 (Proved in [Corlay et al. \(2019\)](#)) *Consider a lattice defined by a VR or a SVR basis $\mathcal{B} = \{b_i\}_{i=1}^n$. Suppose that the $n-1$ points $\mathcal{B} \setminus \{b_1\}$ belong to the hyperplane $\{y \in \mathbb{R}^n : y \cdot e_1 = 0\}$. Then, the decision boundary is given by a CPWL function $f : \mathbb{R}^{n-1} \rightarrow \mathbb{R}$, expressed as*

$$f(\tilde{y}) = \wedge_{m=1}^M \{\vee_{k=1}^{l_m} g_{m,k}(\tilde{y})\}, \quad (4)$$

where $g_{m,k} \in \mathcal{H}$, $1 \leq l_m < \tau_f$, and $1 \leq M \leq 2^{n-1}$.

From now on, **the default orientation of the basis with respect to the canonical axes of \mathbb{R}^n is assumed to be the one of Theorem 2**. We call f the decision boundary function. The domain of f (its input space) is $\mathcal{D}(\mathcal{B}) \subset \mathbb{R}^{n-1}$. The domain $\mathcal{D}(\mathcal{B})$ is the topological closure of the projection of $\mathcal{P}(\mathcal{B})$ on the hyperplane $\{e_i\}_{i=2}^n$. It is a bounded polyhedron that can be partitioned into convex (and thus connected) regions which we call linear regions. For any \tilde{y} in one of these regions, f is described by a unique local affine function h_j . The number of those regions is equal to the number of affine pieces of f .

In the sequel, L denotes the number of layers in the neural network evaluating the boundary function f defined on $\mathcal{D}(\mathcal{B})$ and w is the network width. Also, $\mathcal{N}(f)$ gives the number of pieces of a CPWL function f .

3. (In)approximability results for A_n

Consider a basis for the lattice A_n with all vectors from the first lattice shell. Also, the angle between any two basis vectors is $\pi/3$. Let J_n denote the $n \times n$ all-one matrix and I_n the identity matrix. The Gram matrix is

$$\Gamma_{A_n} = GG^T = J_n + I_n. \quad (5)$$

Assume that one is only given k pieces to build a function g approximating f , with $k < \mathcal{N}(f)$. What is the minimum possible approximation error?

The decision boundary function f for A_2 is illustrated on Figure 1 by the thick yellow line. This function is the same triangle wave function as the one used to prove the main separation theorem between deep and shallow networks in [Telgarsky \(2016\)](#). We quickly recall the main ideas of his proof (a more detailed explanation is also available in Appendix B). A triangle wave function f with p periods is considered. It has $2p + 1$ affine pieces. Telgarsky established a lower bound of the average pointwise disagreement $|f(\tilde{y}) - g(\tilde{y})|$ over a compact set between this function and a function g having k pieces where $k < 2p + 1$. This is achieved by summing the triangle areas above (resp. below) the dashed black line (see Figure 1 or Figure 8) whenever g is below (resp. above) this same line. Indeed, since g has a limited number of pieces, it can only cross this line a limited number of times.

Now, what happens if we consider a similar function in \mathbb{R}^3 , where we replace triangles by tetrahedra? Such a function, limited to $\mathcal{D}(B)$, is illustrated on Figure 2. It is the decision boundary obtained for A_3 defined by (5). The dashed line of Figure 1 should now be replaced by the plane $\Phi^{n=3} = \{y \in \mathbb{R}^3 : y \cdot e_1 = \frac{1}{2} \times (b_1 \cdot e_1)\}$. Similarly to the triangle wave function, $f^{n=3}$

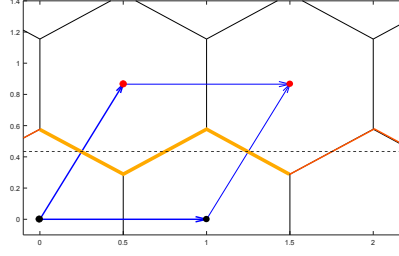


Figure 1: $\mathcal{P}(\mathcal{B})$ for A_2 . The thick blue arrows represent the basis. The CPWL boundary function f defined on $\mathcal{D}(\mathcal{B})$ is illustrated by the thick yellow line. The corner points in $\mathcal{C}^1_{\mathcal{P}(\mathcal{B})}$ are in red and the corner points in $\mathcal{C}^0_{\mathcal{P}(\mathcal{B})}$ are in black. f can also be extended to a larger compact set (the thin red lines).

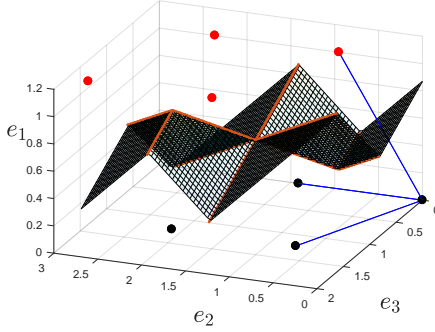


Figure 2: CPWL decision boundary function for A_3 . The basis vectors are represented by blue lines. The corner points in $\mathcal{C}^1_{\mathcal{P}(\mathcal{B})}$ are in red and the corner points in $\mathcal{C}^0_{\mathcal{P}(\mathcal{B})}$ in black.

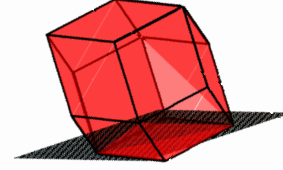


Figure 3: The Voronoi cell of A_3 is a rhombic dodecahedron. A subset of the facets of this polytope generates some affine pieces of f . The non-truncated tetrahedron is the part of the dodecahedron below the plane $\Phi^{n=3}$.

is oscillating around $\Phi^{n=3}$: all pieces of $f^{n=3}$ cross $\Phi^{n=3}$. Note that the number of pieces is significantly increased compared to a simple extension of the triangle wave function in \mathbb{R}^3 (see e.g. Figure 9). Another figure with $\Phi^{n=3}$ cutting $f^{n=3}$ is available in Appendix E. The same pattern is observed for any space dimension n , where the triangles or tetrahedra become n -simplices.

Consider any convex part of f , say $f_m = \vee_{k=1}^m g_{m,k}$ (see (4)). There are 2^{n-1} of such f_m . The polytope

$$\{y \in \mathcal{P}(\mathcal{B}) : y_1 \geq f_m(\tilde{y}), y \cdot e_1 \leq \frac{1}{2} \times (b_1 \cdot e_1)\}$$

is a truncated simplex due to the limitation of f to $\mathcal{D}(\mathcal{B})$. For all m , $1 \leq m \leq 2^{n-1}$, these polytopes are the truncated version of a n -simplex. This simplex is illustrated for $n = 3$ on Figure 3.

This same function can be extended to \mathbb{R}^n by periodicity, i.e. same boundary in $\mathcal{P}(\mathcal{B}) + x$ as in $\mathcal{P}(\mathcal{B})$, for any lattice point x . Indeed, $\mathcal{P}(\mathcal{B})$ is a fundamental region of the lattice and one can perform a tessellation of \mathbb{R}^n with $\mathcal{P}(\mathcal{B})$. This translates into extending the boundary function of (4) as follows: $f(\tilde{y}_0) = f(\tilde{y})$ where $y = y_0 - x \in \mathcal{P}(\mathcal{B})$. We consider a set $\mathcal{P}(\{b_1, \alpha b_2, \alpha b_3, \dots, \alpha b_n\})$, where $\alpha = 2^M$ and $M \geq 1$ is an integer. The new scaled region has $2^{M(n-1)}$ copies of $\mathcal{P}(\mathcal{B})$. This

extended function is defined over the domain $\mathcal{D}(\{b_1, \alpha b_2, \alpha b_3, \dots, \alpha b_n\})$, which is the projection of the scaled region on the hyperplane $\{e_i\}_{i=2}^n$. If we let M grow with n , the exponential increase of the volume yields a total number of pieces superexponential in n . The next proposition, showing that this extended function can be efficiently computed by a deep and narrow network, is constructively proved in Appendix C.1.

Proposition 3 *Consider a VR or SVR basis \mathcal{B} defining any lattice and its extended decision boundary function defined on the compact set $\mathcal{D}(\{b_1, \alpha b_2, \alpha b_3, \dots, \alpha b_n\})$, where $\alpha = 2^M$. Then, the boundary function has $\Omega(2^{M(n-1)})$ pieces and it can be computed by a ReLU network of width $\max(3(n-1), w)$ and depth $3M + L$ (where L and w are the parameters of the neural network evaluating f on $\mathcal{D}(\mathcal{B})$).*

The boundary function f limited to $\mathcal{D}(\mathcal{B})$ and its extension to $\mathcal{D}(\{b_1, \alpha b_2, \alpha b_3, \dots, \alpha b_n\})$ are used to prove approximability and inapproximability results for shallow networks.

Theorem 4 *Consider an A_n -lattice basis defined by the Gram matrix (5). Let f be the decision boundary function.*

1. *Suppose that (5) is scaled by $(n+1)^{-1/n}$ to get $\text{Vol}(\mathcal{P}(\mathcal{B})) = 1$. If f is defined on the compact set $\mathcal{D}(\mathcal{B})$, there exists an affine function h represented as a linear network with one neuron such that:*

$$\lim_{n \rightarrow \infty} \|f - h\|_1 = \lim_{n \rightarrow \infty} \int_{\mathcal{D}(\mathcal{B})} |f(\tilde{y}) - h(\tilde{y})| d\tilde{y} = 0. \quad (6)$$

2. *Let f be defined on the compact set $\mathcal{D}(\{b_1, \alpha b_2, \alpha b_3, \dots, \alpha b_n\})$, where $\alpha = 2^M$ and $\|b_i\| = \sqrt{2}$, $1 \leq i \leq n$. For M large enough, any function g that can be computed by a L -deep, w -wide ReLU neural network where $L \log_2(w) \leq M - n$ has an error*

$$\|f - g\|_1 = \Omega\left(2^{(n-1)M - n \log_2(n)}\right), \quad (7)$$

whereas if $L = 3M + \mathcal{O}(n^2)$ and $w = 3(n-1)$, f can be computed by the network.

Sketch of proof 1. Assume that there are K distinct truncated simplices of the form $\{y \in \mathcal{P}(\mathcal{B}) : y_1 \geq f_m(\tilde{y}), y \cdot e_1 \leq \frac{1}{2} \times (b_1 \cdot e_1)\}$ or $\{y \in \mathcal{P}(\mathcal{B}) : y_1 \leq f_m(\tilde{y}), y \cdot e_1 \geq \frac{1}{2} \times (b_1 \cdot e_1)\}$. The L_1 difference between f and the function h_Φ , defined by the hyperplane $\Phi = \{y \in \mathbb{R}^n : y \cdot e_1 = \frac{1}{2} \times (b_1 \cdot e_1)\}$, is bounded from above by the volume of K non-truncated simplices. Under $\text{Vol}(\mathcal{P}(\mathcal{B})) = 1$, the volume of a non-truncated simplex is bounded from above by $1/n!$. There are $K = 2^n$ distinct truncated simplices in $\mathcal{P}(\mathcal{B})$. Hence, the upper-bound is asymptotic to $\frac{1}{\sqrt{2\pi n} 2^{n \log_2(n/e) - n}}$.

2. We begin with the first part of the second result. The volume of a non-truncated simplex is $\Omega(1/n^n)$. If $\mathcal{P}(\{b_1, \alpha b_2, \alpha b_3, \dots, \alpha b_n\})$ is large enough, there are at least as many non-truncated simplex as instance of $\mathcal{P}(\mathcal{B})$ in the large compact set: i.e. $2^{M(n-1)}$. The result is then achieved by using the fact that no L -deep w -wide ReLU network with input in \mathbb{R}^{n-1} can compute more than $\mathcal{O}(2^{(n-1)L \log_2(w)})$ pieces, combined with the “crossing” argument of Telgarsky (2016).

The second part of the result is a direct consequence of Proposition 3, where the part of f on $\mathcal{D}(\mathcal{B})$ is evaluated via folding with $\mathcal{O}(n^2)$ reflections. The formal proof is available in Appendix C.2. ■

Corollary 5 Consider an A_n -lattice basis defined by the Gram matrix (5). Let $y \in \mathcal{P}(\mathcal{B})$ be drawn from a uniform distribution over $\mathcal{P}(\mathcal{B})$. The average error, when decoding the first coordinate z_1 of y via the sign of the projection of y on the normal vector to Φ , is $\epsilon < \frac{1}{\sqrt{2\pi n 2^n \log_2(n/e) - n}}$.

Note that, despite the first result of Theorem 4 and Corollary 5, for medium dimensions, there may be an interest to add pieces to the function g approximating f on $\mathcal{D}(\mathcal{B})$. Indeed, the decrease in the approximation error might be too slow for some applications (e.g. in communications error rates of at least 10^{-5} are expected) and could be speed up via additional pieces. The second result of the theorem is interesting only for networks of small or medium depth as the size of the compact set should increase exponentially for the inapproximability to hold.

On the other hand, if the size of the compact set is fixed, any shallow network can approximate the boundary function f for A_n due to the decrease in $1/n!$ of the volume of a n -simplex. Hence, we need more sophisticated functions to illustrate the benefit of neural networks and depth in this situation. We present such functions in the next section.

4. Folding-based neural decoding of D_n and E_n

We introduce three new CPWL functions. For each function, we proceed as follows.

1. We count the number of pieces of the function defined on $\mathcal{D}(\mathcal{B})$. It is shown to be exponential in the space dimension.
2. We prove that the function can be efficiently computed via *folding*: i.e. we perform a quadratic number of reflections on $\tilde{y} \in \mathcal{D}(\mathcal{B})$ as pre-processing. After folding, the function can be evaluated by computing a linear number of affine pieces.
3. We then rely on the strategy detailed in Appendix D (presented in Corlay et al. (2019)) to show how this translates into a ReLU neural network of depth increasing linearly with the number of reflections and a width that is linear in the dimension.

The study of approximation of these functions by shallower networks is not provided in this section and left for future work. However, we conjecture that their more complex structure makes them harder to be approximated than the function of the previous section. Hence, they could potentially be used to show gap theorems without using the oscillatory/periodic construction.

4.1. D_n with the basis of Construction A

D_n can be generated from the parity check code via Construction A (Conway and Sloane (1999)). This leads to a basis where the angle between any two vectors is $\pi/3$. Also, all vectors have the same length, except one which has twice the length of the others. This basis is not VR but SVR. The Gram matrix is:

$$\Gamma_{D_n}^{(1)} = \begin{pmatrix} 4 & 2 & 2 & \dots & 2 \\ 2 & 2 & 1 & \dots & 1 \\ 2 & 1 & 2 & \dots & 1 \\ \vdots & \vdots & \vdots & \dots & \vdots \\ 2 & 1 & 1 & \dots & 2 \end{pmatrix}. \quad (8)$$

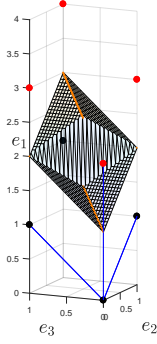


Figure 4: CPWL decision boundary function for D_3 defined by the basis of Construction A. The basis is rotated: b_1 is collinear with e_1 .

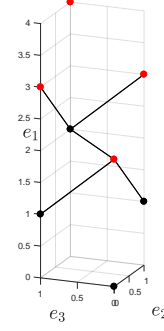


Figure 5: “Neighbor” figure of $\mathcal{C}_{\mathcal{P}(\mathcal{B})}$ for D_3 defined by the basis of Construction A. Each edge connects a point $x \in \mathcal{C}_{\mathcal{P}(\mathcal{B})}^1$ to an element of $\tau_f(x) \cap \mathcal{C}_{\mathcal{P}(\mathcal{B})}^0$. The i edges connected to a point $x \in \mathcal{C}_{\mathcal{P}(\mathcal{B})}^1$ are 1-faces of a i -simplex.

Theorem 6 Consider a D_n -lattice basis defined by the Gram matrix (8). The decision boundary function f , defined on $\mathcal{D}(\mathcal{B})$, has a number of affine pieces equal to

$$\sum_{i=0}^{n-2} \underbrace{\left((n-1-i) + \binom{n-1-i}{2} \right)}_{(l)} \times \underbrace{\binom{n-1}{i}}_{(o)}. \quad (9)$$

Sketch of proof We briefly explain what are the (l) and (o) terms in (9). On Figure 5, i -simplices are illustrated. Any i -simplex is defined by a point $x \in \mathcal{C}_{\mathcal{P}(\mathcal{B})}^1$ and the i points taken from $\tau_f(x) \cap \mathcal{C}_{\mathcal{P}(\mathcal{B})}^0$. Any piece of f , depicted in Figure 4, is also a piece of the decision boundary of one of the i -simplices: i.e. this latter boundary is a function separating the only corner of the simplex $x \in \mathcal{C}_{\mathcal{P}(\mathcal{B})}^1$ from the other corners in $\tau_f(x) \cap \mathcal{C}_{\mathcal{P}(\mathcal{B})}^0$. Hence, each distinct i -simplex generates i pieces in f . The number of pieces of f is then obtained by finding the number of i -simplices: e.g. on Figure 5, there are two 1-simplices and one 3-simplex, thus f has 5 pieces. In (9), (l) represents the dimension of a given simplex and (o) the number of such simplices in $\mathcal{P}(\mathcal{B})$. (l) and (o) are found by exploiting the structure of $\mathcal{P}(\mathcal{B})$ as done in Appendix C.3. ■

Given the basis orientation as in Theorem 2, the projection of b_j on $\mathcal{D}(\mathcal{B})$ is b_j itself, $2 \leq j \leq n$. We also denote the bisector hyperplane between two vectors b_j, b_k by $BH(b_j, b_k)$ and its normal vector is taken to be $v_{j,k} = b_j - b_k$. We define the folding transformation $F : \mathcal{D}(\mathcal{B}) \rightarrow \mathcal{D}'(\mathcal{B})$ as follows. Let $\tilde{y} \in \mathcal{D}(\mathcal{B})$, for all $2 \leq j < k \leq n$, compute $\tilde{y} \cdot v_{j,k}$ (the first coordinate of $v_{j,k}$ is zero). If the scalar product is non-positive, replace \tilde{y} by its mirror image with respect to $BH(b_j, b_k)$. There exist $\binom{n-1}{2}$ hyperplanes for mirroring.

Theorem 7 Let us consider the lattice D_n defined by the Gram matrix (8). We have (i) for all $\tilde{y} \in \mathcal{D}(\mathcal{B})$, $f(\tilde{y}) = f(F(\tilde{y}))$ and (ii) f has exactly

$$2n - 1 \quad (10)$$

pieces on $\mathcal{D}'(\mathcal{B})$. This is to be compared with (9).

The folding procedure is identical to the one used for A_n (see [Corlay et al. \(2019\)](#)): the number of pieces to evaluate is reduced to a linear number via $\mathcal{O}(n^2)$ reflections with respect to the bisector hyperplanes between any pair of vectors in $\mathcal{B} \setminus \{b_1\}$. The proof presents no novelty and is deferred to Appendix C.4.

As a result, f can be computed by a ReLU network of depth $\mathcal{O}(n^2)$ and width $\mathcal{O}(n)$ (with the strategy explained in Appendix D).

4.2. Second basis of D_n

We investigate a second basis of D_n . All basis vectors have the same length but we have both $\pi/3$ and $\pi/2$ angles between the basis vectors. This basis is not VR but SVR. It is defined by the following Gram matrix.

$$\Gamma_{D_n}^{(2)} = \begin{pmatrix} 2 & 0 & 1 & \dots & 1 \\ 0 & 2 & 1 & \dots & 1 \\ 1 & 1 & 2 & \dots & 1 \\ \vdots & \vdots & \vdots & \ddots & \vdots \\ 1 & 1 & 1 & \dots & 2 \end{pmatrix}. \quad (11)$$

Theorem 8 *Consider a D_n -lattice basis defined by the Gram matrix (11). The decision boundary function f , defined on $\mathcal{D}(\mathcal{B})$, has a number of affine pieces equal to*

$$\sum_{i=0}^{n-2} \left(\underbrace{[1 + (n-2-i)]}_{(l)} + \underbrace{\left[\underbrace{1 + 2(n-2-i)}_{(1)} + \underbrace{\binom{n-2-i}{2}}_{(2)} \right]}_{(ll)} \right) \times \underbrace{\binom{n-2}{i}}_{(o)} - 1. \quad (12)$$

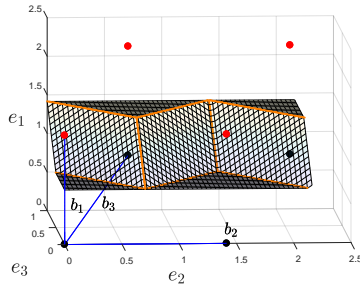


Figure 6: CPWL boundary function for D_3 defined by the second basis. The basis is rotated to better illustrate the symmetry: b_1 is collinear with e_1 .

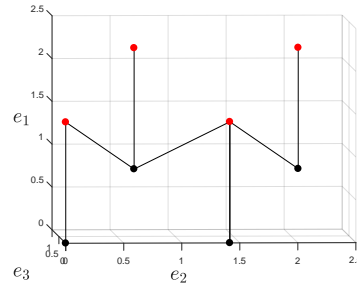


Figure 7: “Neighbor” figure of $\mathcal{C}_{\mathcal{P}(\mathcal{B})}$ for D_3 defined by the second basis.

We give an example to gain insight into the above formula. The proof is deferred to Appendix C.5. The previous sketch of proof highlights that we need to count the i -simplices to get

the number of pieces of f . This is achieved by finding the different “neighborhood patterns” (this gives (l) and (ll)) and counting the occurrence of i -simplices for each of these patterns (this gives (o)). The following example presents the two different patterns encountered with this basis of D_n . In the Appendix, we then count the number of simplices (i.e. (o)) in each of these two categories.

Example 1 Consider the decision boundary function of Figure 6. We are looking for the different “neighborhood patterns” by studying Figure 7: i.e. we are looking for the different ways to find the neighbors of $x \in \mathcal{C}_{\mathcal{P}(\mathcal{B})}^1$ in $\tau_f(x) \cap \mathcal{C}_{\mathcal{P}(\mathcal{B})}^0$, depending on the form of x . In the sequel, (l), (ll), and (1), (2) refer to Equation (12) and $\sum_j b_j$ denotes any sum of points in the set $\{0, b_j\}_{j=3}^n$. We recall that adding b_1 to any point $x \in \mathcal{C}_{\mathcal{P}(\mathcal{B})}^0$ leads to a point in $\mathcal{C}_{\mathcal{P}(\mathcal{B})}^1$.

(l) Firstly, we consider any point in $\mathcal{C}_{\mathcal{P}(\mathcal{B})}^1$ of the form $\sum_j b_j + b_1$. Its neighbors in $\mathcal{C}_{\mathcal{P}(\mathcal{B})}^0$ are $\sum_j b_j$ and any $\sum_j b_j + b_i$, where b_i is any basis vector having an angle of $\pi/3$ with b_1 such that $\sum_j b_j + b_i$ is not outside $\mathcal{P}(\mathcal{B})$. For $n = 3$, the closest neighbors of $0 + b_1$ in $\mathcal{C}_{\mathcal{P}(\mathcal{B})}^0$ are 0 and b_3 . b_2 is perpendicular to b_1 and is not a closest neighbor of b_1 . We get a $1 + n - 2$ -simplex generating 2 pieces f . The point $b_3 + b_1$ also belongs to this category except that no basis vectors having an angle of $\pi/3$ with b_1 can be added to b_3 without leaving $\mathcal{P}(\mathcal{B})$ (i.e. $b_3 + b_3 + b_1$ is not in $\mathcal{P}(\mathcal{B})$). Hence, the only closest neighbor of $b_3 + b_1$ in $\mathcal{C}_{\mathcal{P}(\mathcal{B})}^0$ is b_3 : we have a $1 + n - 2 - 1$ -simplex. Note that this pattern is the same as the (only) one encountered for A_n with the basis given by Equation (5) (see Appendix F).

(ll) The second pattern is obtained with any point of the form $\sum_j b_j + b_2 + b_1$ and its neighbors in $\mathcal{C}_{\mathcal{P}(\mathcal{B})}^0$, where b_2 is the basis vector orthogonal to b_1 . $\sum_j b_j + b_2$ and any $\sum_j b_j + b_2 + b_i$, $\sum_j b_j + b_k$ are neighbors of this point in $\mathcal{C}_{\mathcal{P}(\mathcal{B})}^0$, where b_i, b_k are any basis vector having an angle of $\pi/3$ with b_1 such that (respectively) $\sum_j b_j + b_2 + b_i$, $\sum_j b_j + b_k$ are not outside $\mathcal{P}(\mathcal{B})$. For $n = 3$, the closest neighbors of $0 + b_2 + b_1$ in $\mathcal{C}_{\mathcal{P}(\mathcal{B})}^0$ are b_2 , $b_2 + b_3$, and b_3 . We get a $1 + 2(n - 2)$ -simplex. For $b_3 + b_2 + b_1$, it is the same pattern, except that in this case no b_i can be added to $b_3 + b_2$ without leaving $\mathcal{P}(\mathcal{B})$: we have a $1 + 2(n - 2 - 1)$ -simplex. These terms generate (1) in the formula. Moreover, for $n = 3$ one “neighborhood case” is not happening: from $n = 4$, the points $b_i + b_j \in \mathcal{C}_{\mathcal{P}(\mathcal{B})}^0$, $3 \leq i < j \leq n$, are also closest neighbors of $b_2 + b_1$. This explains the binomial coefficient (2).

Given the basis orientation as in Theorem 2, the folding transformation $F : \mathcal{D}(\mathcal{B}) \rightarrow \mathcal{D}'(\mathcal{B})$ is defined as follows. Let $\tilde{y} \in \mathcal{D}(\mathcal{B})$, for all $3 \leq j < k \leq n$, compute $\tilde{y} \cdot v_{j,k}$ (the first coordinate of $v_{j,k}$ is zero). If the scalar product is non-positive, replace \tilde{y} by its mirror image with respect to $BH(b_j, b_k)$. There exist $\binom{n-2}{2}$ hyperplanes for mirroring.

Theorem 9 Let us consider the lattice D_n defined by the Gram matrix (11). We have (i) for all $\tilde{y} \in \mathcal{D}(\mathcal{B})$, $f(\tilde{y}) = f(F(\tilde{y}))$ and (ii) f has exactly

$$6n - 6 \tag{13}$$

pieces on $\mathcal{D}'(\mathcal{B})$. This is to be compared with (12).

Sketch of proof To count the number of pieces of f , defined on $\mathcal{D}'(\mathcal{B})$, we need to enumerate the cases where both $x \in \mathcal{C}_{\mathcal{P}(\mathcal{B})}^1$ and $x' \in \tau_f(x) \cap \mathcal{C}_{\mathcal{P}(\mathcal{B})}^0$ are on the non-negative side of all reflection hyperplanes. Among the points in $\mathcal{C}_{\mathcal{P}(\mathcal{B})}$ only the points

1. $x_1 = b_3 + \dots + b_{i-1} + b_i$ and $x_1 + b_1$,

$$2. x_2 = b_3 + \dots + b_{i-1} + b_i + b_2 \text{ and } x_2 + b_1,$$

$i \leq n$, are on the non-negative side of all reflection hyperplanes. Via Example 1, it is then easily seen that the number of pieces of f , defined on $\mathcal{D}'(\mathcal{B})$, is given by equation (12) reduced as follows: the three terms $(n - 2 - i)$ (i.e. $2(n - 2 - i)$ counts for two), the term $\binom{n-2-i}{2}$, and the term $\binom{n-2}{i}$ become 1 at each step i , for all $0 \leq i \leq n - 3$ (except $\binom{n-2-i}{2}$ which is equal to 0 for $i = n - 3$). Hence, (12) becomes $(n - 3) \times (2 + 4) + (2 + 3) + 1$, which gives the announced result. ■

Consequently, f can be computed by a ReLU network of depth $\mathcal{O}(n^2)$ and width $\mathcal{O}(n)$ (with the strategy explained in Appendix D).

4.3. E_n

Finally, we investigate E_n , $6 \leq n \leq 8$. E_8 is one of the most famous and remarkable lattices due to its exceptional density relatively to its dimension (it was recently proved that E_8 is the densest packing of congruent spheres in 8-dimensions (Viazovska (2017))). The basis we consider is almost identical to the basis of D_n given by (11), except one main difference: there are two basis vectors orthogonal to b_1 instead of one. This basis is not VR but SVR. It is defined by the following Gram matrix.

$$\Gamma_{E_n} = \begin{pmatrix} 2 & 0 & 0 & 1 & \dots & 1 \\ 0 & 2 & 1 & 1 & \dots & 1 \\ 0 & 1 & 2 & 1 & \dots & 1 \\ 1 & 1 & 1 & 2 & \dots & 1 \\ \vdots & \vdots & \vdots & \vdots & \dots & \vdots \\ 1 & 1 & 1 & 1 & \dots & 2 \end{pmatrix}. \quad (14)$$

Theorem 10 Consider an E_n -lattice basis, $6 \leq n \leq 8$, defined by the Gram matrix (11). The decision boundary function f , defined on $\mathcal{D}(\mathcal{B})$, has a number of affine pieces equal to

$$\sum_{i=0}^{n-3} \left(\underbrace{[1 + (n - 3 - i)]}_{(l)} + 2 \underbrace{\left[1 + 2(n - 3 - i) + \binom{n-3-i}{2} \right]}_{(ll)} + \underbrace{\left[\underbrace{1 + 3(n - 3 - i)}_{(1)} + 3 \underbrace{\binom{n-3-i}{2}}_{(2)} + \underbrace{\binom{n-3-i}{3}}_{(3)} \right]}_{(lll)} \right) \underbrace{\binom{n-3}{n-i}}_{(o)} - 3. \quad (15)$$

Sketch of proof We first highlight the similarities with the function of D_n defined by (11) (we use the same numbering as in the in Example 1). As with D_n , we have case (l). Case (ll) of D_n is also present but obtained twice because of the two orthogonal vectors. The terms $n - 2 - i$ in (l) and (ll) of Equation (12) are replaced by $n - 3 - i$ also because of the additional orthogonal vector.

There is a new pattern (lll): any point of the form $\sum_j b_j + b_3 + b_2 + b_1$ and its neighbors in $\mathcal{C}_{\mathcal{P}(\mathcal{B})}^0$, where $\sum_j b_j$ represents any sum of points in the set $\{0, b_j\}_{j=4}^n$. For instance, the closest neighbors in $\mathcal{C}_{\mathcal{P}(\mathcal{B})}^0$ of $b_3 + b_2 + b_1 \in \mathcal{C}_{\mathcal{P}(\mathcal{B})}^1$ are the following points, which we can sort in three groups as on Equation (15): (1) $b_2 + b_j, b_3 + b_j, b_2 + b_3 + b_j$, (2) $b_j + b_k, b_2 + b_j + b_k, b_3 + b_j + b_k$, (3) $b_j + b_i + b_k, 4 \leq i < j < k \leq n$. The formal proof is available in Appendix C.7. ■

Given the basis orientation as in Theorem 2, the folding transformation $F : \mathcal{D}(\mathcal{B}) \rightarrow \mathcal{D}'(\mathcal{B})$ is defined as follows. Let $\tilde{y} \in \mathcal{D}(\mathcal{B})$, for all $4 \leq j < k \leq n$ and $j = 2, k = 3$, compute $\tilde{y} \cdot v_{j,k}$ (the first coordinate of $v_{j,k}$ is zero). If the scalar product is non-positive, replace \tilde{y} by its mirror image with respect to $BH(b_j, b_k)$. There exist $\binom{n-3}{2}+1$ hyperplanes for mirroring. We get the following theorem, whose proof is available in Appendix C.8.

Theorem 11 *Let us consider the lattice E_n , $6 \leq n \leq 8$, defined by the Gram matrix (8). We have (i) for all $\tilde{y} \in \mathcal{D}(\mathcal{B})$, $f(\tilde{y}) = f(F(\tilde{y}))$ and (ii) f has exactly*

$$12n - 40 \tag{16}$$

pieces on $\mathcal{D}'(\mathcal{B})$. This is to be compared with (15).

Consequently, f can be computed by a ReLU network of depth $\mathcal{O}(n^2)$ and width $\mathcal{O}(n)$ (with the strategy explained in Appendix D).

References

- R. Arora, A. Basu, P. Mianjy, and A. Mukherjee. Understanding deep neural networks with rectified linear units. *International Conference on Learning Representations*, 2018.
- J. Conway and N. Sloane. *Sphere packings, lattices and groups*. Springer-Verlag, 1999.
- V. Corlay, J.J. Boutros, P. Ciblat, and L. Brunel. Neural lattice decoders. *6th IEEE Global Conference on Signal and Information Processing*, also available at: *arXiv preprint arXiv:1703.02930*, Dec. 2018.
- V. Corlay, J.J. Boutros, P. Ciblat, and L. Brunel. On the cvp for the root lattices via folding with deep relu neural networks. *Submitted to 2019 IEEE International Symposium on Information Theory*, also available at www.josephboutros.org/isit2019lattices.pdf, Jan. 2019.
- H. Coxeter. *Regular Polytopes*. 3rd edition, 1973.
- A. Daniely. Depth separation for neural networks. *34th Annual Conference on Learning Theory*, pages 690–696, 2017.
- R. Eldan and O. Shamir. The power of depth for feedforward neural networks. *29th Annual Conference on Learning Theory*, page 907940, 2016.
- T. Gruber, S. Cammerer, J. Hoydis, and S. ten Brink. On deep learning-based channel decoding. *Conference on Information Sciences and Systems*, March 2017.
- G. Montùfar, R. Pascanu, K. Cho, and Y. Bengio. On the number of linear regions of deep neural networks. *Advances in neural information processing systems*, pages 2924–2932, 2014.
- E. Nachmani, E. Marciano, L. Lugosch, W.J. Gross, D. Burshtein, and Y. Be’ery. Deep learning methods for improved decoding of linear codes. *IEEE Journal of Selected Topics in Signal Processing*, 12:119–131, Feb. 2018.
- P. Petersen and F. Voigtlaender. Optimal approximation of piecewise smooth functions using deep relu neural networks. *Neural Networks, Elsevier*, 108:296–330, Dec. 2018.
- T. Poggio, H. Mhaskar, L. Rosasco, B. Miranda, and Q. Liao. Why and when can deep but not shallow networks avoid the curse of dimensionality: a review. *Center for Brains, Minds and Machines (CBMM) Memo No. 58*, 2017.
- M. Raghu, B. Poole, J. Kleinberg, S. Ganguli, and J. Sohl-Dickstein. On the expressive power of deep neural networks. *arXiv preprint arXiv:1606.05336*, June 2016.
- I. Safran and O. Shamir. Depth-width tradeoffs in approximating natural functions with neural networks. *34th Annual Conference on Learning Theory*, pages 2979–2987, 2017.
- M. Telgarsky. Benefits of depth in neural networks. *29th Annual Conference on Learning Theory*, page 15171539, 2016.
- M. Viazovska. The sphere packing problem in dimension 8. *Annals of Mathematics*, 185(2): 9911015, 2017.

Appendix A. Recent results on the expressive power of deep neural networks

The ultimate goal of research on the expressive power of deep neural networks is to find a large function class that can only be addressed via deep neural networks and no other ways, including shallow networks and “conventional approaches” (i.e. not deep neural networks). Results of research works in this field are usually either capacity bounds (i.e. what can do a deep neural network) or separation bounds. These bounds can depend on (i) the approximation error, (ii) the dimension of the input as well as (iii) the width and (iv) the depth of the neural network.

Unfortunately, results on larger function class tend to be looser as the bounds have to hold for the worst-case scenario. Moreover, one of the (empirically observed) strength of neural networks compared to other techniques is their ability to efficiently approximate a given function. Therefore, stronger theorems can be obtained for specific functions but are less representative.

Consequently, papers in the literature can be sorted based on the “size” of the function class addressed and whether or not the results depend on (i),(ii),(iii), and (iv). The present work addresses a small function class (even though it may be a starting point to study algebraic functions), (i), (ii), (iii) and (iv). The following list is not exhaustive and does not include older results related to the field of circuit complexity.

[Eldan and Shamir \(2016\)](#) proved a separation theorem including (i), (ii), and (iii) for a large class of function, namely “radial” functions. Nevertheless, this separation holds only for two-layer and three-layer neural networks, thus (iv) is missing. Also, note that [Daniely \(2017\)](#) found a simpler proof of this result and [Safran and Shamir \(2017\)](#) extended this separation result between two-layer and three-layer network to a larger class of function including the Euclidean unit ball.

[Montufar et al. \(2014\)](#) achieved the best capacity theorem for deep ReLU neural networks including (ii), (iii), and (iv). Similarly to our work, this is achieved via a small function class. As shown in the Appendix of [Corlay et al. \(2019\)](#), these functions can be computed via conventional methods as they are based on a periodic one dimensional function.

[Telgarsky \(2016\)](#) proved a separation theorem between shallow and deep networks (this separation theorem was improved by [Arora et al. \(2018\)](#) by re-using the same ideas) including (i), (iii) and (iv). Since this theorem is based on a one dimensional triangle wave function (see Appendix B), (ii) is missing (a multi-dimensional function is considered but the bound does not depend on (ii)).

[Arora et al. \(2018\)](#) achieved a multi-dimensional construction with an exponential number of linear regions requiring only a polynomial number of parameters (part (i) of Theorem 3.9 in the paper) but the proof is based on the fact that the high dimensional part of this function can be computed by a conventional method (i.e. the function with w^n pieces considered can be computed via a w 2-max, as shown in the proof of Lemma 3.7).

[Raghu et al. \(2016\)](#) showed that any random deep ReLU network achieves an exponential number of linear region depending on (ii),(iii) and (iv). Additionally, via the trajectory length, they observed that most of the random linear regions in trained networks are in fact noise that should be addressed through regularization.

Finally, [Poggio et al. \(2017\)](#) and [Petersen and Voigtlaender \(2018\)](#) are recent results addressing large function class.

Appendix B. The triangle wave function of [Telgarsky \(2016\)](#)

Telgarsky considers a one dimensional triangle wave function. The key observation is that adding two (shifted) copies of a triangle wave function increases the number of pieces in an additive manner,

while composition acts multiplicatively. Within a neural network, increasing the width of a layer is equivalent to adding functions, while increasing the depth is equivalent to composing functions. Hence, a function computed by a deep network, say $f : \mathbb{R} \rightarrow \mathbb{R}$, can have many more oscillations than functions computed by networks with few layers, say $g : \mathbb{R} \rightarrow \mathbb{R}$. Roughly speaking, if the activation function in each neuron is a triangle wave function with p pieces, a two-layer w -wide network leads to a triangle wave function of wp pieces while a L layers network with $\mathcal{O}(1)$ -width leads to p^L pieces.

The difference (or “error”) between f and a line can be characterized by the triangle areas illustrated on Figure 8. Hence, the L^1 error between f and g is then bounded from below after summing the triangle areas above the line (resp. below the line) whenever g is below (resp. above) this same line. Indeed, since g has a number of pieces inferior to f , it can only cross this line a limited number of times compared to f .

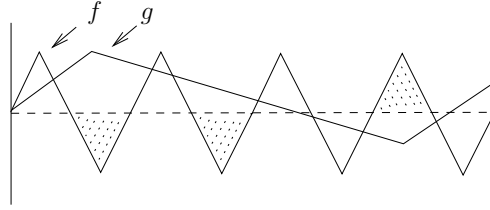


Figure 8: Triangle wave function considered by Telgarsky. The dotted triangle areas are used to get a lower bound of the error between f and g .

This one-dimensional result is then extended to the n -dimensional case in the following manner. A function $p_{\tilde{y}}(y_1) = (y_1, \tilde{y})$ is defined. \tilde{y} can be understood as an offset. The network is then only applied on y_1 but the error averaged in the cube $[0, 1]^n$.

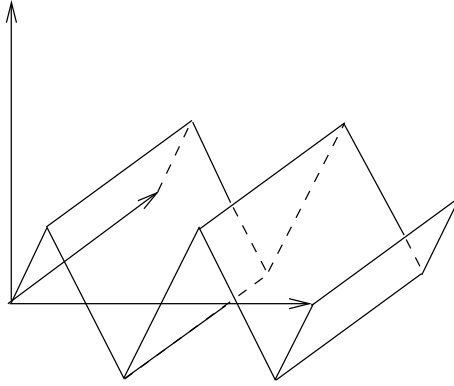


Figure 9: Triangle wave function with offset in \mathbb{R}^3 . The number of pieces is not increased compared to the baseline function in \mathbb{R}^2 . There is no dimensional dependence.

Appendix C. Deferred proofs

C.1. Proof of Proposition 3: a function with a superexponential number of pieces over a large compact set

Proof First, let us define (without loss of generality) the 2-sawtooth ReLU activation function as $\text{ReLU}(u) = u \bmod 1, \forall u \in [0, 2]$. This function allows to divide any interval into two equal sub-intervals and then translates the point near the origin. For illustration in \mathbb{R}^2 , as shown in Figures 10&11, (y_1, y_2) is multiplied by G^{-1} , the 2-sawtooth ReLU is applied twice (on each coordinate), the output is subtracted from the other output to implement the floor operation, and then the result is multiplied again by G . This corresponds to partitioning $\mathcal{P}(2\mathcal{B})$ into four equal regions $\{\mathcal{P}(\mathcal{B}), \mathcal{P}(\mathcal{B}) + b_1, \mathcal{P}(\mathcal{B}) + b_2, \mathcal{P}(\mathcal{B}) + b_1 + b_2\}$.

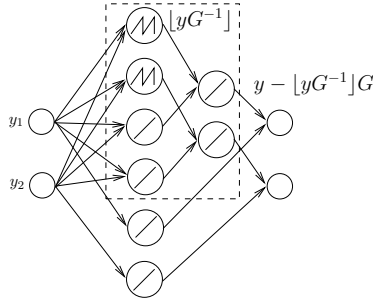


Figure 10: Translation block.

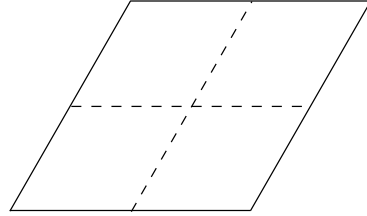


Figure 11: Partition of $\mathcal{P}(2\mathcal{B})$ induced by one translation block.

In \mathbb{R}^n , the 2-sawtooth ReLU is used to partition and translate $\mathcal{P}(\alpha\mathcal{B})$, where $\alpha = 2^M$ and $M \geq 1$ is an integer. At step ℓ , $\ell = 1 \dots M$, a translation block similar to Figure 10 executes the three operations: multiply by $G/2^{M-\ell}$, apply n times a 2-sawtooth ReLU, finally multiply by $2^{M-\ell}G$. $\mathcal{P}(\alpha\mathcal{B})$ has $\alpha^n = 2^{Mn}$ regions equivalent to $\mathcal{P}(\mathcal{B})$. Similarly, if we consider the set $\mathcal{P}(\{b_1, \alpha b_2, \alpha b_3, \dots, \alpha b_n\})$, there are $2^{M(n-1)}$ regions equivalent to $\mathcal{P}(\mathcal{B})$ and the extended decision boundary function defined on the domain $\mathcal{D}(\{b_1, \alpha b_2, \alpha b_3, \dots, \alpha b_n\})$ has $\Omega(2^{M(n-1)})$ pieces.

Hence, the extended boundary function is computed via two neural networks: a first neural network with $3M$ layers based on M translation blocks of maximum width $3(n-1)$ converts $y_0 \in \mathcal{P}(\{b_1, \alpha b_2, \alpha b_3, \dots, \alpha b_n\})$ into $y \in \mathcal{P}(\mathcal{B})$. Subsequently, the second neural network, evaluating f defined on $\mathcal{D}(\mathcal{B})$, takes y as its input. ■

Note that this result brings very little novelty as it is very similar to the results of Montùfar et al. (2014) (we established a link between the function they use and Construction A in the Appendix of Corlay et al. (2019)) as well as to the one-dimensional composition argument used by Telgarsky (2016) (see Appendix B). Moreover, it hardly justifies the superiority of deep neural networks as this operation can be handled by any conventional method.

C.2. Proof of Theorem 4

C.2.1. PROOF OF 1.

To prove 1, we compute an upper bound of the L_1 difference between f and the function h_Φ defined by the hyperplane $\Phi = \{y \in \mathbb{R}^n : y \cdot e_1 = \frac{1}{2} \times (b_1 \cdot e_1)\}$. We show that this bound goes to 0 for large n . It is then obvious that an affine function can be implemented via a one-neuron linear network.

Proof Let $\mathcal{S}(\mathcal{B}_s \cup \{0\})$ denote the non-truncated n -simplex (illustrated in Figure 3 for $n = 3$), defined by a basis \mathcal{B}_s . The first step is to prove that all polytopes $\{y \in \mathcal{P}(\mathcal{B}) : y_1 \geq f_m(\tilde{y}), y \cdot e_1 \leq \frac{1}{2} \times (b_1 \cdot e_1)\}$, $\{y \in \mathcal{P}(\mathcal{B}) : y_1 \leq f_m(\tilde{y}), y \cdot e_1 \geq \frac{1}{2} \times (b_1 \cdot e_1)\}$ are indeed truncated versions of $\mathcal{S}(\mathcal{B}_s \cup \{0\})$ and that there are $K = 2^n$ distinct versions of them in $\mathcal{P}(\mathcal{B})$. We rely essentially on the proof of Theorem 4 in Corlay et al. (2019) (available in Appendix F): this proof shows that there are $\sum_{i=1}^n \binom{n-1}{n-i} = 2^{n-1}$ distinct convex regions in f . Since for any convex region there is a corresponding concave region, there are 2^n of such polytopes. This same proof also shows that the facets of any of these polytopes (except the facets lying in Φ or in a facet of $\mathcal{P}(\mathcal{B})$) are orthogonal to 1-faces of a regular i -simplex (this simplex is not $\mathcal{S}(\mathcal{B}_s \cup \{0\})$), $1 \leq i \leq n$, where all these simplices have one 1-face collinear with a vector defined by x and $x + b_1$, $x \in \mathcal{C}_{\mathcal{P}(\mathcal{B})}^0$ (see Figure 15 for the 3-dimensional case). Hence, all these polytopes are truncated version of the same part of the Voronoi cell of A_n and thus of $\mathcal{S}(\mathcal{B}_s \cup \{0\})$.

The second step is to get an upper bound of the volume of each truncated simplex. Clearly, it is inferior to the volume of the non-truncated regular n -simplex $\mathcal{S}(\mathcal{B}_s \cup \{0\})$. What is the volume of $\mathcal{S}(\mathcal{B}_s \cup \{0\})$? This volume is upper-bounded by $\text{Vol}(\mathcal{P}(\mathcal{B}))/n!$ (see Subsection C.2.3 below).

Finally, the L_1 distance between f and h_Φ is bounded from above by the sum of the volumes of $K \mathcal{S}(\mathcal{B}_s \cup \{0\})$. If we take $\text{Vol}(\mathcal{P}(\mathcal{B})) = 1$, we get

$$\int_{\mathcal{D}} |f(\tilde{y}) - h_\Phi(\tilde{y})| d\tilde{y} < 2^n \cdot \frac{\text{Vol}(\mathcal{P}(\mathcal{B}))}{n!} \sim \frac{1}{\sqrt{2\pi n} 2^{n \log_2(n/e) - n}}, \quad (17)$$

where we used Stirling's approximation. ■

C.2.2. PROOF OF 2.

Proof We begin with the first part of the second result. If the compact set $\mathcal{P}(\{b_1, \alpha b_2, \alpha b_3, \dots, \alpha b_n\})$, where $\alpha = 2^M$, is large enough, we can make the following approximation: there are roughly as many Voronoi cell as parallelotopes $\mathcal{P}(\mathcal{B})$ in $\mathcal{P}(\{b_1, \alpha b_2, \alpha b_3, \dots, \alpha b_n\})$. This implies that the extended decision boundary f “contains” at least one non-truncated simplex for each $\mathcal{P}(\mathcal{B})$. With Proposition 3, we get that there are $2^{M(n-1)} \mathcal{P}(\mathcal{B})$ in $\mathcal{P}(\{b_1, \alpha b_2, \alpha b_3, \dots, \alpha b_n\})$. The volume of one non-truncated simplex is $\Omega(1/n^n)$ for an edge length of $\sqrt{2}$ (see Subsection C.2.3 below). Hence, if K is the number of $\mathcal{P}(\mathcal{B})$ in $\mathcal{P}(\{b_1, \alpha b_2, \alpha b_3, \dots, \alpha b_n\})$, the error between f and g is bounded from below by

$$\int_{\mathcal{D}} |f(\tilde{y}) - g(\tilde{y})| d\tilde{y} = K \Omega(1/n^n), \quad (18)$$

where $K = 2^{M(n-1)} = 2^{M(n-1) - n \log_2(n)} \cdot 2^{n \log_2(n)}$.

Similarly to the strategy of Telgarsky (see Appendix B), we can assume that each additional piece in g cancels (at most) the volume of $\mathcal{O}(1)$ simplices in the bound. Moreover, via Theorem 1

of [Raghu et al. \(2016\)](#) we know that no L -deep w -wide ReLU network with input in \mathbb{R}^{n-1} can compute more than $\mathcal{O}(2^{(n-1)L \log_2(w)})$ pieces. Consequently, the approximation error is bounded from below by

$$a \times 2^{(n-1)(M - \log_2(n)) - \log_2(n)} - b \times 2^{(n-1)L \log_2(w)}, \quad (19)$$

where a and b are some constants. As a result, if we choose $M \geq L \log_2(w) + n$, then the approximation error is $\Omega(2^{(n-1)M - n \log_2(n)})$.

The second part of the result is a direct consequence of Proposition 3, where the part of f on $\mathcal{D}(\mathcal{B})$ is evaluated as follows: we implement the $\mathcal{O}(n^2)$ reflections, that enable to reduce the number of pieces to compute down to a linear number, via a ReLU neural network of depth $\mathcal{O}(n^2)$ and width $\mathcal{O}(n)$ (see Theorem 5 in [Corlay et al. \(2019\)](#) or Section 4). ■

C.2.3. VOLUME OF THE NON-TRUNCATED SIMPLEX

In this subsection, we show that the volume of the non-truncated simplex has a lower bound that behaves as $1/n^n$ and an upper bound given by $\text{Vol}(\mathcal{P}(\mathcal{B}))/n!$.

Let V_n be the volume of the non-truncated simplex described in Section 3. This simplex is equivalent to a hyperpyramid obtained by intersecting $V(0)$ with the hyperplane Φ orthogonal to e_1 and located at a shift of $\frac{1}{2}b_1 \cdot e_1$. Figure 12 illustrates the volume V_n in pink color. The blue color represents the regular simplex whose vertices are $\{0, \frac{1}{2}b_1, \frac{1}{2}b_2, \dots, \frac{1}{2}b_n\}$.

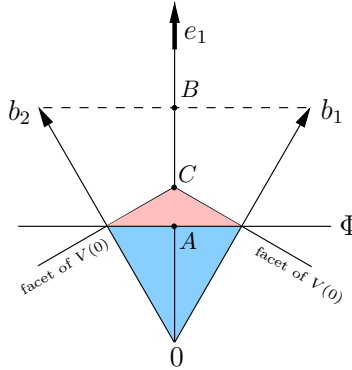


Figure 12: Illustration of the non-truncated simplex (in pink on the figure).

The volume of the hyperpyramid is $V_n = \frac{S \times h}{n}$, where S is the $n - 1$ -dimensional volume of this hyperpyramid facet lying on Φ and h is the hyperpyramid height.

We start by determining h . Let O be the point representing the origin in \mathbb{R}^n . Denote by C the centroid of the regular simplex whose vertices are $\{0, b_1, b_2, \dots, b_n\}$. The line OC cuts Φ at the point A and the hyperplane $\{b_i\}_{i=1}^n$ at the point B . Then $h = OC - OA$ becomes

$$h = OC - \frac{1}{2}OB = \frac{n}{n+1}OB - \frac{1}{2}OB = \frac{n-1}{2(n+1)}\sqrt{\frac{n+1}{n}},$$

because $OB = \sqrt{\frac{n+1}{n}}$ is the height of the regular simplex with edge length $\sqrt{2}$. The area S , i.e. the $n - 1$ -dimensional volume of the facet lying on Φ , is bounded from below by the area S' of the blue

simplex facet lying on Φ . Figure 12 shows them equal in \mathbb{R}^2 , but the facet of the pink simplex will be larger than its blue counterpart for $n \geq 3$. From the formula of a regular simplex volume, we get

$$S \geq S' = \frac{a^{n-1}}{(n-1)!} \frac{\sqrt{n}}{2^{(n-1)/2}}, \quad a = \frac{1}{2} \|b_1\| = \frac{1}{\sqrt{2}}.$$

Finally, the lower bound of V_n is

$$\begin{aligned} V_n &\geq \frac{S' \times h}{n} = \frac{n(n-1)}{2^n \times (n+1)^{3/2} \times n!} \\ &\sim \frac{1}{\sqrt{2\pi}} \frac{1}{(2n/e)^n}. \end{aligned}$$

Hence, the volume of the non-truncated simplex is $\Omega(1/n^n)$.

Moreover, the vectors defined by n points of the simplex and their intersections generate a parallelotope. This parallelotope is included in $\mathcal{P}(\mathcal{B})$, its volume is thus inferior to the one of $\mathcal{P}(\mathcal{B})$. The volume of any simplex is $n!$ times smaller than the volume of the parallelotope generated by the n points. Hence, the volume of the non-truncated simplex is bounded from above by $\text{Vol}(\mathcal{P}(\mathcal{B}))/n!$.

C.3. Proof of Theorem 6: number of pieces of f with the basis of Construction A of D_n

This proof follows the same logic as the proof of the boundary function for A_n (presented in Corlay et al. (2019) and available in Appendix F).

Proof We recall that any piece of f is located in a hyperplane orthogonal to a segment joining a point $x \in \mathcal{C}_{\mathcal{P}(\mathcal{B})}^1$ and one of its neighbors $x' \in \tau_f(x) \cap \mathcal{C}_{\mathcal{P}(\mathcal{B})}^0$. For a given point in $\mathcal{C}_{\mathcal{P}(\mathcal{B})}^1$, the neighbors of interest can be found via the following property of this basis of D_n :

$$\begin{aligned} \forall x \in \mathcal{C}_{\mathcal{P}(\mathcal{B})}^0, x' \in D_n \setminus \{b_j, 0\} \setminus \{b_j + b_j\}, 2 \leq i < j \leq n : \\ \{x + b_j\} \setminus \{x\} \in \tau_f(x + b_1), \{x + b_i + b_j\} \setminus \{x\} \in \tau_f(x + b_1), \\ x + x' \notin \tau_f(x + b_1) \cap \mathcal{C}_{\mathcal{P}(\mathcal{B})}^0. \end{aligned} \quad (20)$$

In other words, the two main differences with A_n are that (i) summing two basis vectors $b_i + b_j \in \mathcal{C}_{\mathcal{P}(\mathcal{B})}^0$, $2 \leq i < j \leq n$, results in a point which is a closest neighbor of $b_1 \in \mathcal{C}_{\mathcal{P}(\mathcal{B})}^1$ and (ii) $x \in \mathcal{C}_{\mathcal{P}(\mathcal{B})}^0$ is not a closest neighbor of $x + b_1$. This clearly appears on Figure 5. A point $x \in \mathcal{C}_{\mathcal{P}(\mathcal{B})}^1$ and its neighbors $\tau_f(x) \cap \mathcal{C}_{\mathcal{P}(\mathcal{B})}^0$ form a $|\tau_f(x) \cap \mathcal{C}_{\mathcal{P}(\mathcal{B})}^0|$ -simplex \mathcal{S} .

Now, consider the decision boundary function of a i -simplex separating the top corner (i.e. $\mathcal{C}_{\mathcal{S}}^1 = \{x\}$, $x \in \mathcal{C}_{\mathcal{P}(\mathcal{B})}^1$) from all the other corners (i.e. $\mathcal{C}_{\mathcal{S}}^0 = \tau_f(x) \cap \mathcal{C}_{\mathcal{P}(\mathcal{B})}^0$). As long as no corner in $\mathcal{C}_{\mathcal{S}}^0$ has its first coordinate e_1 larger than the first coordinate of the top corner, which is always the case with the orientation of the basis as in Theorem 2, the function is convex and has i pieces. The maximal size of such simplex in $\mathcal{P}(\mathcal{B})$ is obtained by taking the point b_1 , the $n-1$ points b_j , $2 \leq j \leq n$, and the $\binom{n-1}{2}$ points $b_i + b_j$, $2 \leq i < j \leq n$. Hence, the decision boundary function f has a number of affine pieces equal to

$$\sum_{i=1}^{n-1 + \binom{n-1}{2}} i \times (\# \text{ } i\text{-simplices}), \quad (21)$$

where, for each i -simplex, only one corner x belongs to $\mathcal{C}_{\mathcal{P}(\mathcal{B})}^1$ and the other corners constitute the set $\tau_f(x) \cap \mathcal{C}_{\mathcal{P}(\mathcal{B})}^0$.

We now count the number of i -simplices. We walk in $\mathcal{C}_{\mathcal{P}(\mathcal{B})}^0$ and for each of the 2^{n-1} points $x \in \mathcal{C}_{\mathcal{P}(\mathcal{B})}^0$ we investigate the size of the simplex where the top corner is $x + b_1 \in \mathcal{C}_{\mathcal{P}(\mathcal{B})}^1$. This is achieved by counting the number of elements in $\tau_f(x + b_1) \cap \mathcal{C}_{\mathcal{P}(\mathcal{B})}^0$, via the property given by (20). Starting from the origin, one can form a $n - 1 + \binom{n-1}{2}$ -simplex with the point b_1 , the $n - 1$ points b_j , $2 \leq j \leq n$, and the $\binom{n-1}{2}$ points $b_i + b_j$, $2 \leq i < j \leq n$. Then, from any b_{j_1} , $2 \leq j_1 \leq n$, one can only use the $n - 1$ remaining basis vectors to generate a simplex in $\mathcal{P}(\mathcal{B})$. Indeed, if we add again b_{j_1} , the resulting point (i.e. the point $b_{j_1} + b_{j_1}$, which is a neighbor of $b_{j_1} + b_1$) is outside $\mathcal{P}(\mathcal{B})$ and should therefore not be considered. Hence, we get a $(n - 1) - 1 + \binom{n-1-1}{2}$ -simplex and there are $\binom{n-1}{1}$ ways to choose b_{j_1} : any basis vector except b_1 . Similarly, if one starts the simplex from $b_{j_1} + b_{j_2}$, one can form a $(n - 1) - 2 + \binom{n-1-2}{2}$ -simplex in $\mathcal{P}(\mathcal{B})$ and there are $\binom{n-1}{2}$ ways to choose $b_{j_1} + b_{j_2}$. In general, there are $\binom{n-1}{i}$ ways to form a $n - 1 - i + \binom{n-1-i}{2}$ -simplex. ■

C.4. Proof of Theorem 7: folding of f with the basis of Construction A of D_n

Lemma 12 *Among the elements of $\mathcal{C}_{\mathcal{P}(\mathcal{B})}$, only the points of the form $x = b_2 + b_3 + \dots + b_{i-1} + b_i$ and $x + b_1$, $i \leq n$, are on the non-negative side of all $BH(b_j, b_k)$, $2 \leq j < k \leq n$.*

Proof In the sequel, $\sum_i b_i$ denotes any sum of points in the set $\{0, b_i\}_{i=2}^n$. First, consider a point of the form $b_2 + b_3 + \dots + b_{j-1} + b_{j+1} + \dots + b_{i-1} + b_i$, $j + 1 < i - 1 \leq n - 1$. This point is on the negative side of all $BH(b_j, b_k)$, $j < k \leq i$. More generally, any point $\sum_i b_i$, where $\sum_i b_i$ includes in the sum b_k but not b_j , $j < k \leq n$, is on the negative side of $BH(b_j, b_k)$. Hence, the only points in $\mathcal{C}_{\mathcal{P}(\mathcal{B})}^0$ that are on the non-negative side of all hyperplanes have the form $b_2 + b_3 + \dots + b_{i-1} + b_i$, $i \leq n$.

Moreover, if $x \in \mathcal{C}_{\mathcal{P}(\mathcal{B})}^0$ is on the negative side of one of the hyperplanes $BH(b_j, b_k)$, $2 \leq j < k \leq n$, so is $x + b_1$ since b_1 is in all $BH(b_j, b_k)$. ■

Proof (of Theorem 7) (i) is the direct result of the symmetries in the D_n -lattice basis where the $n - 1$ vectors $\{b_j\}_{j=2}^n$ form a regular $n - 1$ -dimensional simplex. The folding via $BH(b_j, b_k)$ switches b_j and b_k in the hyperplane containing $\mathcal{D}(\mathcal{B})$. $\mathcal{D}(\mathcal{B})$ is orthogonal to both e_1 and $BH(b_j, b_k)$, $2 \leq j < k \leq n$. Switching b_j and b_k does not change the decision boundary because of the basis symmetry, hence f is unchanged.

Now, for (ii), how many pieces are left after all reflections? To count the number of pieces of f , defined on $\mathcal{D}'(\mathcal{B})$, we need to enumerate the cases where both $x \in \mathcal{C}_{\mathcal{P}(\mathcal{B})}^1$ and $x' \in \tau_f(x) \cap \mathcal{C}_{\mathcal{P}(\mathcal{B})}^0$ are on the non-negative side of all reflection hyperplanes. Hence, for any given point $x \in \mathcal{C}_{\mathcal{P}(\mathcal{B})}^0$, that is on the proper side of all reflection hyperplanes, we count the number of elements in $\tau_f(x + b_1) \cap \mathcal{C}_{\mathcal{P}(\mathcal{B})}^0$ (via Equation (20)) that are also on the proper side of all bisector hyperplanes.

Starting from the origin, due to Lemma 12, one can only form a 2-simplex with b_1 , b_2 , and $b_2 + b_3$: any other point b_j , $3 \leq j \leq n$, is on the negative side of $BH(b_2, b_j)$ and any point $b_j + b_k$, $2 \leq j < k \leq n$, except $b_2 + b_3$, is on the negative side of at least one $BH(b_i, b_j)$, $i \neq j$. In general, due to Lemma 12, all points in $\mathcal{C}_{\mathcal{P}(\mathcal{B})}^1$ that are on the non-negative side of all hyperplanes, have the form $x = b_2 + b_3 + \dots + b_{i-1} + b_i + b_1$, $i \leq n$. There are n of them. For any $1 \leq i \leq n - 1$, x has

only two neighbors in $\mathcal{C}_{\mathcal{P}(\mathcal{B})}^0$ on the non-negative side of all hyperplanes: $x - b_1$ and $x + b_{i+1} - b_1$ (for $i = n$, $x + b_{i+1} - b_1$ is outside $\mathcal{P}(\mathcal{B})$ and x has only one neighbor in $\mathcal{C}_{\mathcal{P}(\mathcal{B})}^0$). As a result, f , defined on $\mathcal{D}'(\mathcal{B})$, has $(n - 1) \times 2 + 1$ pieces. \blacksquare

C.5. Proof of Theorem 8: number of pieces of f with the second basis of D_n

Proof Similarly to the proof of Theorem 6, we count the number of simplices. The number of pieces of f is then obtained by summing the number of pieces of the boundary function of each simplex.

Hence, we walk in $\mathcal{C}_{\mathcal{P}(\mathcal{B})}^0$ and for each of the 2^{n-1} points $x \in \mathcal{C}_{\mathcal{P}(\mathcal{B})}^0$, we investigate the size of the simplex where the top corner is $x + b_1 \in \mathcal{C}_{\mathcal{P}(\mathcal{B})}^1$. This is achieved by counting the number of elements in $\tau_f(x + b_1) \cap \mathcal{C}_{\mathcal{P}(\mathcal{B})}^0$. In this scope, the points in $\mathcal{C}_{\mathcal{P}(\mathcal{B})}^0$ can be sorted into two categories: (I) and (II). In the sequel, $\sum_j b_j$ denotes any sum of points in the set $\{0, b_j\}_{j=3}^n$. These two categories and their properties, illustrated in Example 1 (see also Equation (24) below), are:

$$(I) \forall x = \sum_j b_j \in \mathcal{C}_{\mathcal{P}(\mathcal{B})}^0, x' \in D_n \setminus \{b_k, 0\}, 3 \leq k \leq n : \quad (22)$$

$$x + b_k \in \tau_f(x + b_1), x + x' \notin \tau_f(x + b_1) \cap \mathcal{C}_{\mathcal{P}(\mathcal{B})}^0.$$

$$(II) \forall x = \sum_j b_j + b_2 \in \mathcal{C}_{\mathcal{P}(\mathcal{B})}^0, x' \in D_n \setminus \{b_i, -b_2 + b_i, -b_2 + b_i + b_k, 0\}, 3 \leq i < k \leq n : \quad (23)$$

$$(1) (a) x + b_i \in \tau_f(x + b_1), (b) x - b_2 + b_i \in \tau_f(x + b_1),$$

$$(2) x - b_2 + b_i + b_k \in \tau_f(x + b_1),$$

$$(3) x + x' \notin \tau_f(x + b_1) \cap \mathcal{C}_{\mathcal{P}(\mathcal{B})}^0.$$

We count the number of i -simplices per category.

(I) is like A_n (see Appendix F). Starting from the origin, one can form a $n - 1$ -simplex with 0 , b_1 , and the $n - 2$ other basis vectors except b_2 (because it is perpendicular to b_1). Then, from any b_{j_1} , $3 \leq j_1 \leq n$, one can only add (to b_{j_1}) the $n - 2$ remaining basis vectors (i.e. neither b_1 nor b_{j_1}) to generate a simplex in $\mathcal{P}(\mathcal{B})$ where the top corner is $b_{j_1} + b_1$. Indeed, if we add again b_{j_1} , the resulting point is outside $\mathcal{P}(\mathcal{B})$ and should not be considered. Hence, we get a $n - 2$ -simplex and there are $\binom{n-2}{1}$ ways to choose b_{j_1} : any basis vector except b_1 and b_2 . Similarly, if one starts the simplex from $b_{j_1} + b_{j_2}$, one can form a $n - 3$ -simplex in $\mathcal{P}(\mathcal{B})$ and there are $\binom{n-2}{2}$ ways to choose $b_{j_1} + b_{j_2}$. In general, there are $\binom{n-2}{i}$ ways to form a $n - 1 - i$ -simplex.

(II) To begin with, we are looking for the neighbors of $b_2 + b_1$. First (i.e. property (1)), we have the following $1 + 2 \times (n - 2)$ points in $\tau_f(b_2 + b_1) \cap \mathcal{C}_{\mathcal{P}(\mathcal{B})}^0$: b_2 , any $b_j + b_2$, $3 \leq j \leq n$, and any b_j , $3 \leq j \leq n$. Second (i.e. property (2)), the $\binom{n-2}{2}$ points $b_j + b_k$, $3 \leq j < k \leq n$, are also neighbors of $b_2 + b_1$. Hence, $b_2 + b_1$ has $1 + 2 \times (n - 2) + \binom{n-2}{2}$ neighbors in $\mathcal{C}_{\mathcal{P}(\mathcal{B})}^0$. Then, the points $b_1 + b_2 + b_{j_1}$, $3 \leq j_1 \leq n$, have $1 + 2 \times (n - 2 - 1) + \binom{n-2-1}{2}$ neighbors of this kind, using the same arguments, and there are $\binom{n-2}{1}$ ways to choose b_{j_1} . In general, there are $\binom{n-2}{i}$ ways to form a $1 + 2 \times (n - 2 - i) + \binom{n-2-i}{2}$ - simplex.

To summarize, each pattern replicates $\sum_i \binom{n-2}{i}$ times, where at each step i the patterns yield respectively (l) $1 + (n - 2 - i)$ -simplices and (ll) $1 + 2 \times (n - 2 - i) + \binom{n-2-i}{2}$ -simplices. As a result, the total number of pieces of f is obtained as

$$\sum_{i=0}^{n-2} \left(\underbrace{[1 + (n - 2 - i)]}_{(l)} + \underbrace{\left[\underbrace{1 + 2(n - 2 - i)}_{(1)} + \underbrace{\binom{n-2-i}{2}}_{(2)} \right]}_{(ll)} \right) \times \underbrace{\binom{n-2}{i}}_{(o)} - 1, \quad (24)$$

where the -1 comes from the fact that for $i = n-2$, the piece generated by (l) and the piece generated by (ll) are the same. Indeed, the bisector hyperplane of x , $x + b_1$ and the bisector hyperplane of $x + b_2$, $x + b_2 + b_1$ are the same since b_2 and b_1 are perpendicular. ■

C.6. Proof of Theorem 9: folding of f with the second basis of D_n

Lemma 13 *Among the elements of $\mathcal{C}_{\mathcal{P}(\mathcal{B})}$, only the points of the form*

1. $x_1 = b_3 + \dots + b_{i-1} + b_i$ and $x_1 + b_1$,
2. $x_2 = b_3 + \dots + b_{i-1} + b_i + b_2$ and $x_2 + b_1$,

$i \leq n$, are on the non-negative side of all $BH(b_j, b_k)$, $3 \leq j < k \leq n$.

Proof See the proof of Lemma 12. ■

Proof (of Theorem 9) (i) The folding via $BH(b_j, b_k)$, $3 \leq j < k \leq n$, switches b_j and b_k in the hyperplane containing $\mathcal{D}(\mathcal{B})$, which is orthogonal to e_1 . Switching b_j and b_k does not change the decision boundary because of the basis symmetry, hence f is unchanged.

Now, for (ii), how many pieces are left after all reflections? To count the number of pieces of f , defined on $\mathcal{D}'(\mathcal{B})$, we need to enumerate the cases where both $x \in \mathcal{C}_{\mathcal{P}(\mathcal{B})}^1$ and $x' \in \tau_f(x) \cap \mathcal{C}_{\mathcal{P}(\mathcal{B})}^0$ are on the non-negative side of all reflection hyperplanes.

Firstly, we investigate the effect of the folding operation on the term $\sum_{i=0}^{n-2} [1 + (n - 2 - i)] \times \binom{n-2}{i}$ in Equation (24). Remember that it is obtained via (l) (i.e. Equation (22)). Due to the reflections, among the points in $\mathcal{C}_{\mathcal{P}(\mathcal{B})}^1$ of the form $\sum_j b_j + b_1$ only $x = b_3 + b_4 + \dots + b_{i-1} + b_i + b_1$, $j \leq n$, is on the non-negative side of all reflection hyperplanes (see result 1. of Lemma 13). Similarly, among the elements in $\tau_f(x) \cap \mathcal{C}_{\mathcal{P}(\mathcal{B})}^0$, only $x - b_1$ and $x - b_1 + b_{i+1}$ (instead of $x - b_1 + b_k$, $3 \leq k \leq n$) are on the non-negative side of all reflection hyperplanes. Hence, at each step i , the term $[1 + (n - 2 - i)]$ becomes 2 (except for $i = n - 2$ where it is 1). Therefore, the folding operation reduced the term $\sum_{i=0}^{n-2} [1 + (n - 2 - i)] \times \binom{n-2}{i}$ to $(n - 2) \times 2 + 1$.

Secondly, we investigate the reduction of the term $\sum_{i=0}^{n-2} \left[1 + 2(n - 2 - i) + \binom{n-2-i}{2} \right] \times \binom{n-2}{i}$ obtained via (ll) (i.e. Equation 23). The following results are obtained via item 2. of Lemma 13. Among the points denoted by $\sum_j b_j + b_2 + b_1 \in \mathcal{C}_{\mathcal{P}(\mathcal{B})}^1$ only $x = b_3 + b_4 + \dots + b_{i-1} + b_i + b_2 + b_1$ is on the proper side of all reflection hyperplanes. Among the neighbors of any of these points, of the

form $(ll) - (2)$, only $x + b_{i+1} + b_{i+2}$ is on the proper side of all hyperplanes. Additionally, among the neighbors of the form $(ll) - (1)$ and $(ll) - (b)$, i.e. $x + b_k$ or $x - b_2 + b_k$, $3 \leq k \leq n$, b_k can only be b_{i+1} . Therefore, the folding operation reduces the term $\sum_{i=0}^{n-2} [1 + 2(n-2-i) + \binom{n-2-i}{2}] \times \binom{n-2}{i}$ to $(n-3) \times 4 + 3 + 1$. ■

C.7. Proof of Theorem 10: number of pieces of f for E_n

Proof Similarly to the proof of Theorem 12, we count the number of simplices and investigate their size. The number of pieces of f is then obtained by summing the number of pieces of the boundary functions of each simplex (again, see the proof of Theorem 6). This is achieved by counting the number of elements in $\tau_f(x + b_1) \cap \mathcal{C}_{\mathcal{P}(\mathcal{B})}^0$, for all $x \in \mathcal{C}_{\mathcal{P}(\mathcal{B})}^0$. In this scope, we group the lattice points $x \in \mathcal{C}_{\mathcal{P}(\mathcal{B})}^0$ within three categories. The numbering of these categories matches the one given in the sketch of proof (see also Equation 29 below). $\sum_j b_j$ denotes any sum of points in the set $\{0, b_j\}_{j=4}^n$.

$$(l) : \forall x = \sum_j b_j \in \mathcal{C}_{\mathcal{P}(\mathcal{B})}^0, x' \in D_n \setminus \{b_j, 0\}, 4 \leq k \leq n : \quad (25)$$

$$x + b_k \in \tau_f(x + b_1), x + x' \notin \tau_f(x + b_1) \cap \mathcal{C}_{\mathcal{P}(\mathcal{B})}^0.$$

$$(ll) - A \forall x = \sum_j b_j + b_2 \in \mathcal{C}_{\mathcal{P}(\mathcal{B})}^0, x' \in D_n \setminus \{b_i, -b_2 + b_i, -b_2 + b_i + b_k, 0\}, 4 \leq i < k \leq n : \quad (26)$$

$$\begin{aligned} (1) & x + b_i \in \tau_f(x + b_1), x - b_2 + b_i \in \tau_f(x + b_1), \\ (2) & x - b_2 + b_i + b_k \in \tau_f(x + b_1), \\ (3) & x + x' \notin \tau_f(x + b_1) \cap \mathcal{C}_{\mathcal{P}(\mathcal{B})}^0. \end{aligned}$$

$$(ll) - B \forall x = \sum_j b_j + b_3 \in \mathcal{C}_{\mathcal{P}(\mathcal{B})}^0, x' \in D_n \setminus \{b_i, -b_3 + b_i, -b_3 + b_i + b_k, 0\}, 4 \leq i < k \leq n : \quad (27)$$

$$\begin{aligned} (1) & x + b_i \in \tau_f(x + b_1), x - b_3 + b_i \in \tau_f(x + b_1), \\ (2) & x - b_3 + b_i + b_k \in \tau_f(x + b_1), \\ (3) & x + x' \notin \tau_f(x + b_1) \cap \mathcal{C}_{\mathcal{P}(\mathcal{B})}^0. \end{aligned}$$

$$\begin{aligned}
(III) \quad & \forall x = \sum_j b_j + b_2 + b_3 \in \mathcal{C}_{\mathcal{P}(\mathcal{B})}^0, x' \in D_n \setminus \{b_i, b_i + b_k, b_i + b_k + b_l, 0\}, 4 \leq i < k < l \leq n : \\
& (1) \quad x - b_2 + b_k \in \tau_f(x + b_1), \quad x - b_3 + b_k \in \tau_f(x + b_1), \quad x + b_k \in \tau_f(x + b_1), \\
& (2) \quad x - b_3 - b_2 + b_i + b_k \in \tau_f(x + b_1), \\
& \quad x - b_2 + b_i + b_k \in \tau_f(x + b_1), \quad x - b_3 + b_i + b_k \in \tau_f(x + b_1), \\
& (3) \quad x + b_i + b_k + b_l \in \tau_f(x + b_1), \\
& (4) \quad x + x' \notin \tau_f(x + b_1) \cap \mathcal{C}_{\mathcal{P}(\mathcal{B})}^0.
\end{aligned} \tag{28}$$

We count the number of i -simplices per category.

(I) is like A_n (see Appendix F). Starting from the origin, one can form a $n - 2$ -simplex with 0 , b_1 , and the $n - 2$ other basis vectors except b_2 and b_3 (because they are perpendicular to b_1). Then, from any b_{j_1} , $4 \leq j_1 \leq n$, one can only add (to b_{j_1}) the $n - 3$ remaining basis vectors to generate a simplex in $\mathcal{P}(\mathcal{B})$ where the top corner is $b_{j_1} + b_1$. Indeed, if we add again b_{j_1} , the resulting point (i.e. $b_{j_1} + b_{j_1}$) is outside $\mathcal{P}(\mathcal{B})$. Hence, we get a $n - 3$ -simplex and there are $\binom{n-3}{1}$ ways to choose b_{j_1} : any basis vector except b_1, b_2, b_3 . Similarly, if one starts the simplex from $b_{j_1} + b_{j_2}$, one can form a $n - 4$ -simplex in $\mathcal{P}(\mathcal{B})$ and there are $\binom{n-3}{2}$ ways to choose $b_{j_1} + b_{j_2}$. In general, there are $\binom{n-3}{i}$ ways to form a $n - 2 - i$ -simplex.

(II) is like the second basis of D_n (see (II) in the proof in Appendix C.5), repeated twice because we now have two basis vectors orthogonal to b_1 instead of one. Hence, we get that there are $\binom{n-3}{i}$ ways to form a $2 \times \left(1 + 2(n - 3 - i) + \binom{n-3-i}{2}\right)$ -simplex.

(III) is the new category. We investigate the neighbors of a given point $x = \sum_j b_j + b_3 + b_2 + b_1$. First (1), any $\sum_j b_j + b_3 + b_2$ is in $\tau_f(x) \cap \mathcal{C}_{\mathcal{P}(\mathcal{B})}^0$. Any $\sum_j b_j + b_2 + b_k$, $\sum_j b_j + b_3 + b_k$, and $\sum_j b_j + b_3 + b_2 + b_k$, where $4 \leq k \leq n$ and $k \notin \{j\}$ are also in $\tau_f(x) \cap \mathcal{C}_{\mathcal{P}(\mathcal{B})}^0$. Hence, there are $3 \times (n - 3 - i)$ of such neighbors, where $i = |\{j\}|$ (in $\sum_j b_j$). Then, (2) any $\sum_j b_j + b_i + b_k$, $\sum_j b_j + b_2 + b_i + b_k$, and $\sum_j b_j + b_3 + b_i + b_k$, where $4 \leq i < k \leq n$ and $i, k \notin \{j\}$, are in $\tau_f(x) \cap \mathcal{C}_{\mathcal{P}(\mathcal{B})}^0$. There are $3 \times \binom{n-3-i}{2}$ possibilities, where $i = |\{j\}|$. Finally (3), any $\sum_j b_j + b_i + b_k + b_l$, $4 \leq i < k < l \leq n$ and $i, k, l \notin \{j\}$ are in $\tau_f(x) \cap \mathcal{C}_{\mathcal{P}(\mathcal{B})}^0$. There are $\binom{n-3-i}{3}$ of them, where $i = |\{j\}|$.

To summarize, each pattern replicates $\sum_i \binom{n-3}{i}$ times, where at each step i the patterns yield (I) $1 + n - 3 - i$ -simplices, (II) $2 \times \left(1 + 2(n - 3 - i) + \binom{n-3-i}{2}\right)$ -simplices, and (III) $1 + 3 \times (n - 3 - i) + 3 \times \binom{n-3-i}{2} + \binom{n-3-i}{3}$ -simplices. As a result, the total number of pieces of f is obtained as

$$\sum_{i=0}^{n-3} \left(\underbrace{\left[1 + (n - 3 - i)\right]}_{(I)} + \underbrace{2 \left[1 + 2(n - 3 - i) + \binom{n-3-i}{2}\right]}_{(II)} + \underbrace{\left[\underbrace{1 + 3(n - 3 - i)}_{(1)} + \underbrace{3 \binom{n-3-i}{2}}_{(2)} + \underbrace{\binom{n-3-i}{3}}_{(3)} \right]}_{(III)} \right) \underbrace{\binom{n-3}{n-i}}_{(o)} - 3, \tag{29}$$

where the -3 comes from the fact that for $i = n - 3$, the four pieces generated by (I), (II), and (III) are the same. Indeed, the bisector hyperplane of x , $x + b_1$, is the same as the one of $x + b_2$, $x + b_2 + b_1$, of $x + b_3$, $x + b_3 + b_1$, and of $x + b_2 + b_3$, $x + b_2 + b_3 + b_1$, since both b_2 and b_3 are perpendicular to b_1 . ■

C.8. Proof of Theorem 11: folding of f for E_n

Lemma 14 Among the elements of $\mathcal{C}_{\mathcal{P}(\mathcal{B})}$, only the points of the form

1. $x_1 = b_4 + \dots + b_{i-1} + b_i$ and $x_1 + b_1$,
2. $x_2 = b_4 + \dots + b_{i-1} + b_i + b_2$ and $x_2 + b_1$,
3. $x_3 = b_4 + \dots + b_{i-1} + b_i + b_2 + b_3$ and $x_3 + b_1$,

$i \leq n$, are on the non-negative side of all $BH(b_j, b_k)$, $4 \leq j < k \leq n$.

Proof See the proof of Lemma 12. ■

Proof (of Theorem 11) (i) The folding via $BH(b_j, b_k)$, $4 \leq j < k \leq n$ and $j = 2, k = 3$, switches b_j and b_k in the hyperplane containing $\mathcal{D}(\mathcal{B})$, which is orthogonal to e_1 . Switching b_j and b_k does not change the decision boundary because of the basis symmetry, hence f is unchanged.

Now, for (ii), how many pieces are left after all reflections? To count the number of pieces of f , defined on $\mathcal{D}'(\mathcal{B})$, we need to enumerate the cases where both $x \in \mathcal{C}_{\mathcal{P}(\mathcal{B})}^1$ and $x' \in \tau_f(x) \cap \mathcal{C}_{\mathcal{P}(\mathcal{B})}^0$ are on the non-negative side of all reflection hyperplane.

Firstly, we investigate the effect of the folding operation on the term $\sum_{i=0}^{n-3} [1 + n - 3 - i] \times \binom{n-3}{i}$ in Equation (29). Remember that it is obtained via (l) (i.e. Equation (25)). Due to result 1 of Lemma 14 and similarly to the corresponding term in the proof of Theorem 9, this term reduces to $(n - 3) \times 2 + 1$.

Secondly, we investigate the reduction of the term $2 \left[1 + 2(n - 3 - i) + \binom{n-3-i}{2} \right] \times \binom{n-3}{i}$, obtained via (ll) (i.e. Equation 26). The following results are obtained via item 2 of Lemma 14. $\binom{n-3}{i}$ reduces to 1 at each step i because in $\mathcal{C}_{\mathcal{P}(\mathcal{B})}^1$, only the points $x = b_2 + b_3 + b_{i-1} + b_i + b_1$ are on the non-negative side of all hyperplanes, $i \leq n$. Then, since any $\sum_j b_j + b_3 + b_1$ is on the negative side of the hyperplane $BH(b_2, b_3)$, (ll) - (B) generates no pieces in f (defined to $\mathcal{D}'(\mathcal{B})$). (ll) - (A) is the same situation as the situation (ll) in the proof of Theorem 9. Hence, the term reduces to $(n - 3) \times (4) + 3 + 1$.

Finally, what happens to the term $\left[1 + 3(n - 3 - i) + 3\binom{n-3-i}{2} + \binom{n-3-i}{3} \right] \binom{n-3}{i}$, obtained via (lll) (i.e. Equation 27)? The following results are obtained via item 3 of Lemma 14. As usual, $\binom{n-3}{i}$ reduces to 1 at each step i . Then, $3(n - 3 - i)$, due to (lll) - (1), becomes 2×1 at each step i because any $x - b_2 + b_k$ (in (lll) - (1)), $k \leq 4 \leq n$, is on the negative side of $BH(b_2, b_3)$. For $x - b_3 + b_k$ and $x + b_k$, only one valid choice of b_k remains at each step i , as explained in the proof of Theorem 9. Regarding the term $3\binom{n-3-i}{2}$, due to (lll) - (2), any point $x - b_2 + b_i + b_k$ (in (lll) - (2)) is on the negative side of $BH(b_2, b_3)$ and at each step i there is only one valid way to chose b_j and b_k for both $x - b_3 - b_2 + b_j + b_k$ and $x - b_3 + b_j + b_k$. Eventually, for the last term due to (lll) - (3) only one valid choice remain at each step i . Therefore, the term due to (lll) is reduced to $(n - 4) \times 6 + 5 + 3 + 1$. ■

Appendix D. From folding to a deep ReLU network

For the sake of simplicity and without loss of generality, in addition to the standard ReLU activation function $\text{ReLU}(a) = \max(0, a)$, we also allow the function $\max(0, -a)$ and the identity as activation functions in the network.

To implement a reflection, one can use the following strategy.

1. Step 1: rotate the axes to have the i -th axis e_i perpendicular to the reflection hyperplane and shift the point (i.e. the i -th coordinate) to have the reflection hyperplane at the origin.
2. Step 2: compute the absolute value of the i -th coordinate.
3. Step 3: do the inverse operation of step 1.

Now consider the ReLU network illustrated in Figure 13. The edges between the input layer and the hidden layer represent the rotation matrix, where the i -th column is repeated twice, and p is a bias applied on the i -th coordinate. Within the dashed square, the absolute value of the i -th coordinate is computed and shifted by $-p$. Finally, the edges between the hidden layer and the output layer represent the inverse rotation matrix. This ReLU network computes a reflection. We call it a reflection block.

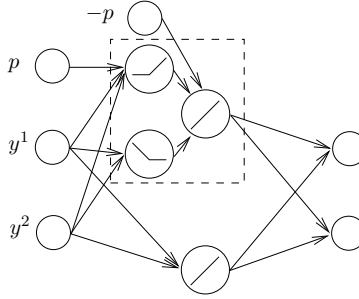


Figure 13: Reflection ReLU network (called reflection block).

All reflections can be naively implemented by a simple concatenation of reflection blocks. Since the $\mathcal{O}(n)$ remaining operations to perform are negligible compared to the previous folding operations (see e.g. Appendix G), the depth of this network increases linearly with the number of reflections and its width is linear in the dimension.

Appendix E. Additional material

The following figure shows the decision boundary function $f^{n=3}$ defined on $\mathcal{D}(B)$ oscillating around the hyperplane $\Phi^{n=3}$. We can also observe the truncated simplices. The black edges on the figure connect a point $x \in \mathcal{C}_{\mathcal{P}(B)}^1$ to an element of $\tau_f(x) \cap \mathcal{C}_{\mathcal{P}(B)}^0$. Any piece of f is orthogonal to one of these edges.

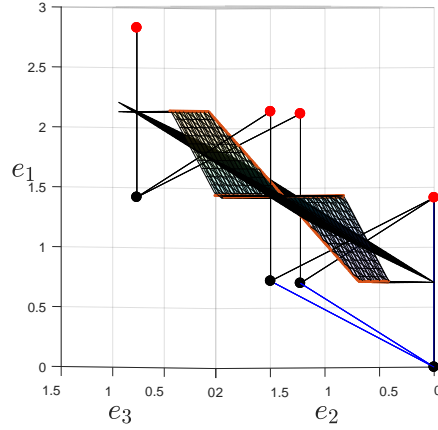


Figure 14: Decision boundary function for A_3 oscillating around the plane $\Phi^{n=3}$.

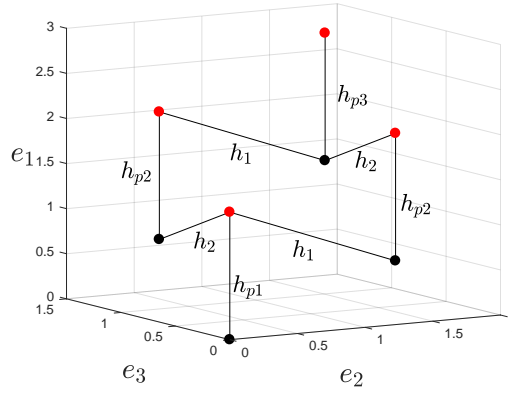


Figure 15: “Neighbor” figure of $\mathcal{C}_{\mathcal{P}(\mathcal{B})}$ for A_3 . Each edge connects a point $x \in \mathcal{C}_{\mathcal{P}(\mathcal{B})}^1$ to an element of $\tau_f(x) \cap \mathcal{C}_{\mathcal{P}(\mathcal{B})}^0$. The i edges connected to a point $x \in \mathcal{C}_{\mathcal{P}(\mathcal{B})}^1$ are 1-faces of a regular i -simplex. The pieces of f are orthogonal to these edges.

Appendix F. Theorem 4 of Corlay et al. (2019) and its proof

The purpose of this part is to count the number of pieces, and thus linear regions, of the decision boundary function f for A_n . We start with the following lemma involving i -simplices, which is then used to prove the following theorem.

Lemma 15 *Consider an A_n -lattice basis defined by the Gram matrix (5). The decision boundary function f has a number of affine pieces equal to*

$$\sum_{i=0}^n i \times (\# \text{ regular } i\text{-simplices}), \quad (30)$$

where, for each i -simplex, only one corner x belongs to $\mathcal{C}_{\mathcal{P}(\mathcal{B})}^1$ and the other corners constitute the set $\tau_f(x) \cap \mathcal{C}_{\mathcal{P}(\mathcal{B})}^0$.

Proof A key property of this basis is

$$\begin{aligned} \forall x \in \mathcal{C}_{\mathcal{P}(\mathcal{B})}^0, x' \in A_n \setminus \{b_j, 0\}, 2 \leq j \leq n : \\ x + b_j \in \tau_f(x + b_1), x + x' \notin \tau_f(x + b_1) \cap \mathcal{C}_{\mathcal{P}(\mathcal{B})}^0. \end{aligned} \quad (31)$$

It is obvious that $\forall x \in \mathcal{C}_{\mathcal{P}(\mathcal{B})}^0: x + b_1 \in \mathcal{C}_{\mathcal{P}(\mathcal{B})}^1$. This implies that any given point $x \in \mathcal{C}_{\mathcal{P}(\mathcal{B})}^1$ and its neighbors $\tau_f(x) \cap \mathcal{C}_{\mathcal{P}(\mathcal{B})}^0$ form a regular simplex \mathcal{S} of dimension $|\tau_f(x) \cap \mathcal{C}_{\mathcal{P}(\mathcal{B})}^0|$. This clearly appears on Figure 15. Now, consider the decision boundary function of a k -simplex separating the top corner (i.e. $\mathcal{C}_{\mathcal{S}}^1$) from all the other corners (i.e. $\mathcal{C}_{\mathcal{S}}^0$). This function is convex and has k pieces. The maximal dimension of such simplex is obtained by taking the points 0, b_1 , and the $n - 1$ points $b_j, j \geq 2$. ■

Theorem 16 Consider an A_n -lattice basis defined by the Gram matrix (5). The decision boundary function f has a number of affine pieces equal to

$$\sum_{i=1}^n i \cdot \binom{n-1}{n-i}. \quad (32)$$

Proof From Lemma 15, what remains to be done is to count the number of k -simplices. We walk in $\mathcal{C}_{\mathcal{P}(\mathcal{B})}^0$ and for each of the 2^{n-1} points $x \in \mathcal{C}_{\mathcal{P}(\mathcal{B})}^0$ we investigate the dimension of the simplex where the top corner is $x + b_1 \in \mathcal{C}_{\mathcal{P}(\mathcal{B})}^1$. This is achieved by counting the number of elements in $\tau_f(x + b_1) \cap \mathcal{C}_{\mathcal{P}(\mathcal{B})}^0$, via the property given by (31). Starting from the origin, one can form a n -simplex with 0, b_1 , and the $n - 1$ other basis vectors. Then, from any $b_{j_1}, j_1 \neq 1$, one can only add the $n - 1$ remaining basis vectors to generate a simplex in $\mathcal{P}(\mathcal{B})$. Indeed, if we add again b_{j_1} , the point goes outside $\mathcal{P}(\mathcal{B})$. Hence, we get a $n - 1$ -simplex and there are $\binom{n-1}{1}$ ways to choose b_{j_1} : any basis vector except b_1 . Similarly, if one starts the simplex from $b_{j_1} + b_{j_2}$, one can form a $n - 2$ -simplex in $\mathcal{P}(\mathcal{B})$ and there are $\binom{n-1}{2}$ ways to choose $b_{j_1} + b_{j_2}$. In general, there are $\binom{n-1}{k}$ ways to form a $n - k$ -simplex. Applying the previous lemma and summing over $k = n - i = 0 \dots n - 1$ gives the announced result. ■

Appendix G. Computing the $\mathcal{O}(n)$ remaining pieces of f after folding

The remaining pieces of f can be evaluated via $\mathcal{O}(\log(n))$ additional hidden layers. First, compute the $\mathcal{O}(n) \vee$ via $\mathcal{O}(1)$ layers of size $\mathcal{O}(n)$ containing several “max ReLU networks” (see e.g. Figure 3 in Arora et al. (2018)). Then, compute the $n \wedge$ via $\mathcal{O}(\log(n))$ layers.

Appendix H. Additional material on lattices

The Gram matrix is $\Gamma = GG^T = (GQ)(GQ)^T$, where Q is any $n \times n$ orthogonal matrix. All bases defined by a Gram matrix are equivalent modulo rotations and reflections. A lower triangular generator matrix is obtained from the Gram matrix by Cholesky decomposition.

$\mathcal{P}(\mathcal{B})$ and $\mathcal{V}(x)$ are fundamental regions of the lattice: one can perform a tessellation of \mathbb{R}^n with these regions.

The fundamental parallelotope of Λ , defined by a basis \mathcal{B} , is given by

$$\mathcal{P}(\mathcal{B}) = \{y \in \mathbb{R}^n : y = \sum_{i=1}^n \alpha_i g_i, 0 \leq \alpha_i < 1\}. \quad (33)$$

The fundamental volume of Λ is $\det(\Lambda) = |\det(G)| = \text{Vol}(\mathcal{V}(x)) = \text{Vol}(\mathcal{P}(\mathcal{B}))$. The Voronoi cell of x is:

$$\mathcal{V}(x) = \{y \in \mathbb{R}^n : \|y - x\| \leq \|y - x'\|, \forall x' \in \Lambda\}. \quad (34)$$

A surface in \mathbb{R}^n defined by a function g of $n - 1$ arguments is written as $\text{Surf}(g) = \{(g(\tilde{y}), \tilde{y}) \in \mathbb{R}^n : \tilde{y} \in \mathbb{R}^{n-1}\}$.

Definition 17 Let $\mathcal{B} = \{b_i\}_{i=1}^n$ be a basis of Λ . Suppose that the $n - 1$ points $\mathcal{B} \setminus \{b_1\}$ belong to the hyperplane $\{y \in \mathbb{R}^n : y \cdot e_1 = 0\}$. The basis is called *semi-Voronoi-reduced (SVR)* if there exists at least two points $x_1, x_2 \in \mathcal{C}_{\mathcal{P}(\mathcal{B})}^1$ such that $\text{Surf}(\bigvee_{k=1}^{\ell_1} g_{1,k}) \cap \text{Surf}(\bigvee_{k=1}^{\ell_2} g_{2,k}) \neq \emptyset$, where $\ell_1, \ell_2 \geq 1$, $g_{1,k}$ are the facets between x_1 and all points in $\tau_f(x_1) \cap \mathcal{C}_{\mathcal{P}(\mathcal{B})}^0$, and $g_{2,k}$ are the facets between x_2 and all points in $\tau_f(x_2) \cap \mathcal{C}_{\mathcal{P}(\mathcal{B})}^0$.